

D-A253 288



PL-TR-91-2170

**A CONSTRAINED BAYESIAN APPROACH
FOR TESTING TTBT COMPLIANCE**

Mark D. Fisk
Henry L. Gray
Gary D. McCartor
Gregory L. Wilson

Mission Research Corporation
735 State Street
P.O. Box 719
Santa Barbara, CA 93102

6 March 1992

Scientific Report No. 1

Approved for public release; distribution unlimited



PHILLIPS LABORATORY
AIR FORCE SYSTEMS COMMAND
HANSCOM AIR FORCE BASE, MASSACHUSETTS
01731-5000

DTIC
ELECTE
JUN 26 1992
S C D

2

92-16785




92 6 25 022

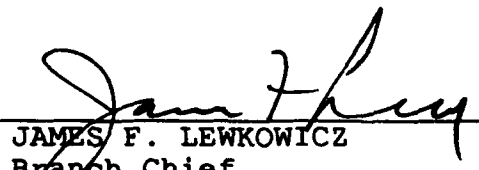
SPONSORED BY
Defense Advanced Research Projects Agency
Nuclear Monitoring Research Office
ARPA ORDER NO. 5307

MONITORED BY
Phillips Laboratory
Contract F19628-90-C-0135

The views and conclusions contained in this document are those of the authors and should not be interpreted as representing the official policies, either expressed or implied, of the Defense Advanced Research Projects Agency or the U.S. Government.

This technical report has been reviewed and is approved for publication.


JAMES F. LEWKOWICZ
Contract Manager
Solid Earth Geophysics Branch
Earth Sciences Division


JAMES F. LEWKOWICZ
Branch Chief
Solid Earth Geophysics Branch
Earth Sciences Division


DONALD H. ECKHARDT, Director
Earth Sciences Division

This report has been reviewed by the ESD Public Affairs Office (PA) and is releasable to the National Technical Information Service (NTIS).

Qualified requestors may obtain additional copies from the Defense Technical Information Center. All others should apply to the National Technical Information Service.

If your address has changed, or if you wish to be removed from the mailing list, or if the addressee is no longer employed by your organization, please notify PL/IMA, Hanscom AFB, MA 01731-5000. This will assist us in maintaining a current mailing list.

Do not return copies of this report unless contractual obligations or notices on a specific document requires that it be returned.

REPORT DOCUMENTATION PAGE			Form Approved OMB No. 0704-0188	
Public reporting burden for this collection of information is estimated to average 1 hour per response, including the time for reviewing instructions, searching existing data sources, gathering and maintaining the data needed, and completing and reviewing the collection of information. Send comments regarding this burden estimate or any other aspect of the collection of information, including suggestions for reducing this burden, to Washington Headquarters Services, Directorate for Information Operations and Reports, 1215 Jefferson Davis Highway, Suite 1204, Arlington, VA 22202-4302, and to the Office of Management and Budget, Paperwork Reduction Project (0704-0188), Washington, DC 20503.				
1. AGENCY USE ONLY (Leave blank)		2. REPORT DATE 920306	3. REPORT TYPE AND DATES COVERED Scientific No. 1	
4. TITLE AND SUBTITLE A CONSTRAINED BAYESIAN APPROACH FOR TESTING TTBT COMPLIANCE			5. FUNDING NUMBERS PE 62714E PR 0A10 TA DA WU AC Contract F19628-90-C-0135	
6. AUTHOR(s) Mark D. Fisk Gregory L. Wilson Henry L. Gray* Gary D. McCartor*				
7. PERFORMING ORGANIZATION NAME(S) AND ADDRESS(ES) Mission Research Corporation P.O. Drawer 719 Santa Barbara, CA 93102-0719			8. PERFORMING ORGANIZATION REPORT NUMBER MRC-R-1367	
9. SPONSORING/MONITORING AGENCY NAME(S) AND ADDRESS(ES) Phillips Laboratory Hanscom Air Force Base Massachusetts 01731-5000 Contract Manager: James Lewkowicz, NH			10. SPONSORING/MONITORING AGENCY REPORT NUMBER PL-TR-91-2170	
11. SUPPLEMENTARY NOTES * Southern Methodist University, Dallas, TX				
12a. DISTRIBUTION/AVAILABILITY STATEMENT Approved for public release; distribution unlimited			12b. DISTRIBUTION CODE	
13. ABSTRACT (Maximum 200 words) A constrained Bayesian approach is applied to the problem of statistically testing TTBT compliance. Our approach allows expert opinion to be used as prior information for the unknown parameters of the yield estimation problem. In addition, we show that existing seismic magnitude data may be used to furnish some information about the unknown parameters even though the associated yields are unknown. That is, since for equal slope parameters, $m_b - m_{Lg}$ does not depend on yield, one can estimate the mean and variance of this difference from data even though the yields are unknown. This information is included in the joint prior distribution in the form of constraints on the difference of the mean and variance parameters of the seismic magnitudes. We investigate the impact of such information on the test of compliance by comparing the power and F-numbers of two tests based on Bayesian approaches, with and without the constraints. We also compare the Bayesian results with those of two tests based on classical statistics. Our formulation treats the intercepts and the covariance matrix of the seismic errors as unknown. To obtain closed form expressions for the power and F-numbers, however, we consider the special case in which the intercepts are treated as random, but the covariance matrix of the seismic errors is treated as known. The comparison shows that the probability of detecting a TTBT violation using the				
14. SUBJECT TERMS Bayesian approach F-number Threshold Test Ban Treaty compliance testing yield estimation			15. NUMBER OF PAGES 64	
			16. PRICE CODE	
17. Security CLASSIFICATION OF REPORT UNCLASSIFIED	18. Security CLASSIFICATION OF THIS PAGE UNCLASSIFIED	19. Security CLASSIFICATION OF ABSTRACT UNCLASSIFIED	20. LIMITATION OF ABSTRACT SAR	

UNCLASSIFIED

SECURITY CLASSIFICATION OF THIS PAGE

CLASSIFIED BY:

DECLASSIFY ON:

constrained Bayesian approach is always at least as great as when using the unconstrained approach. Also, the power of the constrained Bayesian approach is greater than that of a test of hypothesis using only calibration data. The constrained approach is particularly useful when little calibration data is available and there is more uncertainty in one of the intercepts. The results also show that the constrained approach is far more robust, when poor *a priori* information is used, than the unconstrained approach. We discuss how existing magnitude data, for which the yields are unknown, may be used to improve tests of TTBT compliance at calibrated test sites, or to reduce the number of calibration events needed to successfully monitor a new test site.

SECURITY CLASSIFICATION THIS PAGE

UNCLASSIFIED

TABLE OF CONTENTS

Section	Page
1 INTRODUCTION	1
2 NOTATION	3
3 TECHNICAL DEVELOPMENT	5
3.1 Bayesian Approach	5
3.2 The Constrained Prior Distribution	6
3.3 Summary of Technical Developments	8
4 YIELD ESTIMATION AND TESTING COMPLIANCE . .	10
5 POWER COMPARISON	13
6 ROBUSTNESS	19
7 CONCLUSIONS AND FUTURE WORK	24
8 REFERENCES	26



Accession For	
NTIC GRAAI	<input checked="" type="checkbox"/>
DTIC TAB	<input type="checkbox"/>
Unannounced	<input type="checkbox"/>
Justification	
By	
Distribution/	
Availability Codes	
Dist	Avail and/or Special
A-1	

THIS PAGE IS INTENTIONALLY LEFT BLANK

SECTION 1

INTRODUCTION

Over the last two years there has been a growing interest in a Bayesian approach to the problem of testing compliance to the threshold test ban treaty (TTBT). (See Nicholson et al. [1991] and Shumway and Der [1990].) During that same time it has been pointed out that previous data does furnish some information about the unknown parameters in the yield estimation problem even though the associated yields are unknown. For example, since for equal slope parameters, $m_b(P) - m_b(Lg)$ does not depend on yield, one can estimate the mean and variance of this difference from data for which the yields are unknown. Typically, the size of such data sets is large enough to provide excellent estimates of these parameters. This information can then be used to improve estimates of future yields (See Nicholson et al. [1991]).

Our approach is a modification of the approach suggested by Shumway and Der [1990]. They have shown that prior information, supplied for example by a panel of experts, can be useful for improving confidence intervals on the log yield, particularly when there is little calibration data. Our approach also allows expert opinion to be used as prior information. In addition, we include the information gained from previous data for which the yields are unknown, in terms of constraints on the mean and variance of the difference of the seismic magnitudes.

In this report we investigate the effect of such information on a statistical test of TTBT compliance by comparing the power and F-number of the test based on two Bayesian approaches, with and without the constraints. We develop a Bayesian formulation, treating the unknown intercepts and covariance matrix as random variables for which a joint Bayesian prior may be specified, with and without the constraints on the prior. The case in which the slopes are also treated as unknown will be discussed in a subsequent report.

For comparison, we consider a special case in which the covariance matrix is treated as known, without uncertainty, so that expressions for the power and F-numbers may be computed analytically. (This assumption is also made by Nicholson et al. [1991] in their analysis.) A parametric study is performed to assess how the probabilities of detecting violations depend on the true calibration parameters and the number of calibration events for which the yields are known. The results show that when the assumptions of the Bayesian priors (constrained and unconstrained) are correct, the test based on the constrained Bayesian approach has a greater than or

equal probability of detecting a violation (referred to as the power of the test), at the same significance level, than the test without the constraints for all cases examined. The power for the constrained case is particularly greater than the power for the unconstrained case when little calibration data is available and there is considerable uncertainty in one of the intercepts.

We also examine the robustness of the two tests when the Bayesian assumptions are incorrect. That is, we compare the sensitivity of the power functions and false alarm rates of the two tests for monitoring a given test site when the *a priori* assumptions are incorrect, e.g., when the true intercept parameters are out in the tails of the joint prior distribution. Analytic expressions are also given for these probabilities. A discussion of the interpretation of the Bayesian tests for monitoring given test sites is included.

The Bayesian tests are also compared to a test of hypothesis for which all of the calibration parameters are treated as known, and one for which only the intercepts are unknown and estimated strictly from data. The former test provides a reference by which the other tests may be judged. That is, since all of the calibration parameters are known, this test will have the greatest power for fixed significance level. The latter test was considered by Hafemeister [1987]. Comparison with this test allows us to gauge the usefulness of the *a priori* information, including that provided by data for which the yields are unknown.

The remainder of this report is organized as follows. In Section 2 we define the notation of our model. In Section 3 we develop the Bayesian approach, with and without the constraints, and in Section 4 we establish a test of compliance based on these approaches and define the power and the F-number of the test. In Section 5 we present the results of a power comparison between the constrained and unconstrained approaches when the appropriate *a priori* assumptions hold, and in Section 6 we address the issue of robustness. Finally, in Section 7 we draw some conclusions from our study concerning the usefulness of our approach for monitoring specific test sites, and describe future efforts in this area.

SECTION 2

NOTATION

Suppose that there are two seismic magnitudes observed for each event, e.g., $m_i(P)$ and $m_i(Lg)$. Let

m_{ij} = i -th seismic magnitude of the j -th event

W_j = log yield of the j -th event.

Then for constants A_i and B_i , we assume the magnitudes and log yield are related by

$$\begin{aligned} m_{ij} &= A_i + B_i W_j + \epsilon_{ij}; \quad i = 1, 2; \quad j = 1, \dots, n \\ E[\epsilon_{ij}] &= 0 \\ \text{Var } \epsilon_{ij} &= \sigma_{\epsilon_i}^2 \\ \text{Cov}(\epsilon_{1j}, \epsilon_{2j}) &= \rho(\epsilon_1, \epsilon_2) \sigma_{\epsilon_1} \sigma_{\epsilon_2} \end{aligned} \tag{1}$$

We now consider the problem of estimating yield and establishing a compliance test for future events under the following scenario:

The A_i and the covariance matrix of ϵ_{ij} are unknown, but sufficient information is available to define a joint Bayesian prior for these quantities. There are n calibration events for which the yields are known, and the $n + 1$ yield is to be estimated. We also assume the slopes are known, and hence *w.l.o.g.* set $B_1 = B_2 = 1$. (The generalization to other known values of the slopes is straightforward.)

We will also exploit the information contained in previous magnitude data for which the associated yields are unknown. We will hereafter refer to these data sets as "no-yield data." Let

$$E[m_{1j} - m_{2j}] = \mu \tag{2}$$

$$\text{Var}(m_{1j} - m_{2j}) = \lambda^2. \tag{3}$$

Under the assumption that $B_1 = B_2 = 1$, these quantities are independent of the yield. For other values of B_1, B_2 , the appropriate yield-independent combination of the magnitudes is $(B_1^{-1}m_{1j} - B_2^{-1}m_{2j})$. Typically, large no-yield data sets are available which may be used to provide excellent estimates of μ and λ^2 . We will assume for now that such data sets are sufficiently large that the estimated values of μ and λ^2 may be considered to be the actual values.

We now define random variables corresponding to the unknown A_i and the covariance matrix of ϵ_{ij} :

- $\{a_1, a_2\}$ = joint normal random variates, for which we assume the means, μ_{a_1} and μ_{a_2} , variances, $\sigma_{a_1}^2$ and $\sigma_{a_2}^2$, and correlation, ρ_a , are given *a priori*. The means are taken as the "most likely" values of the A_i , and variances and correlation reflect the "best guess" of the uncertainty in our knowledge of the A_i .
- $\{\sigma_1, \sigma_2, \rho\}$ = joint random variates for which we assume sufficient prior information is available to completely specify the probability distribution function (*pdf*). (Several reasonable *pdfs* are specified below.) The prior distribution reflects our uncertainty in the knowledge of σ_{ϵ_1} , σ_{ϵ_2} and $\rho(\epsilon_1, \epsilon_2)$.

We then define

$$m_{ij} = a_i + W_j + \epsilon_{ij}; \quad i = 1, 2; \quad j = 1, \dots, n. \quad (4)$$

We admit that we are abusing the notation here, since m_{ij} in (1) is actually the "conditional" m_{ij} in (4), i.e., given $a_1 = A_1$ and $a_2 = A_2$, and we have failed to make that distinction in our notation. We will also use the same variables a_i , σ_i^2 and ρ to denote the random variables and the values of the random variables. Nevertheless, this should not introduce any confusion. For example, the variables that appear as the arguments of the *pdfs* below will always represent values of the random variables. Also, let

$$\begin{aligned} \mathbf{a} &= \{a_1, a_2\} \\ \boldsymbol{\sigma} &= \{\sigma_1, \sigma_2, \rho\} \\ \vec{m}_k &= (m_{11}, m_{21}, \dots, m_{1k}, m_{2k}), \end{aligned}$$

where we assume that the associated yields are known for $k \leq n$, and unknown for $k = n + 1$.

SECTION 3

TECHNICAL DEVELOPMENT

3.1 Bayesian Approach.

Consider now the problem of determining the joint distribution f of $m_{1,n+1}$ and $m_{2,n+1}$ given \vec{m}_n . This distribution will be used to establish a test of compliance. We may write

$$\begin{aligned} f(m_{1,n+1}, m_{2,n+1} | \vec{m}_n) &= \int f_1(m_{1,n+1}, m_{2,n+1}, a, \sigma | \vec{m}_n) da d\sigma \\ &= \int f_2(m_{1,n+1}, m_{2,n+1} | a, \sigma, \vec{m}_n) f_3(a, \sigma | \vec{m}_n) da d\sigma, \end{aligned} \quad (5)$$

where f_2 and f_3 are functions to be specified. Using Bayes' law, f_3 may be expressed as

$$f_3(a, \sigma | \vec{m}_n) = \frac{h(a, \sigma) L(\vec{m}_n | a, \sigma)}{\int h(a, \sigma) L(\vec{m}_n | a, \sigma) da d\sigma}, \quad (6)$$

where h is the joint prior distribution of a and σ , and L is the likelihood function for the data, \vec{m}_n , given values of a and σ . Note that $(m_{1,n+1}, m_{2,n+1})$ is dependent on \vec{m}_n , as defined by (4), since the random vector (a_1, a_2) is common to both. However, for fixed values of (a_1, a_2) , $(m_{1,n+1}, m_{2,n+1})$ does not explicitly depend on \vec{m}_n . Therefore

$$f_2(m_{1,n+1}, m_{2,n+1} | a, \sigma, \vec{m}_n) = f_2(m_{1,n+1}, m_{2,n+1} | a, \sigma). \quad (7)$$

Assuming (m_{1k}, m_{2k}) are bivariate normal, then

$$f_2(m_{1k}, m_{2k} | a, \sigma) = C \exp \left\{ -\frac{1}{2(1-\rho^2)} (X_k^2 - 2\rho X_k Y_k + Y_k^2) \right\} \equiv \psi(m_{1k}, m_{2k}) \quad (8)$$

for $k = 1, \dots, n$, where

$$C = \frac{1}{2\pi\sigma_1\sigma_2\sqrt{1-\rho^2}}$$

$$X_k = \frac{m_{1k} - W_k - a_1}{\sigma_1}$$

$$Y_k = \frac{m_{2k} - W_k - a_2}{\sigma_2}$$

Using the fact that for given values of (a_1, a_2) , the conditional (m_{1j}, m_{2j}) and (m_{1k}, m_{2k}) are independent for all $j \neq k$, it then follows that

$$L(\vec{m}_n | \mathbf{a}, \sigma) = \prod_{k=1}^n \psi(m_{1k}, m_{2k}). \quad (9)$$

From (5), (6), (8) and (9), $f(m_{1,n+1}, m_{2,n+1} | \vec{m}_n)$ is completely determined if $h(\mathbf{a}, \sigma)$ is available.

Shumway and Der [1990] have derived this expression for $f(m_{1,n+1}, m_{2,n+1} | \vec{m}_n)$. In their formulation, the slopes are also treated as unknown. Thus, \mathbf{a} in our notation would represent the matrix of intercepts and slopes in their scheme. We will depart at this point from their approach and consider the impact, on the corresponding test of hypothesis, of the further assumptions of (2) and (3), where μ and λ^2 are given constants, determined from previous no-yield data.

3.2 The Constrained Prior Distribution.

We impose the constraints (2) and (3) by replacing, in (6), the prior $h(\mathbf{a}, \sigma)$ with a new prior $h_c(\mathbf{a}, \sigma)$. If the mean and variance of the difference are precisely known, then we may take

$$h_c(\mathbf{a}, \sigma) = \mathcal{N} h(\mathbf{a}, \sigma) \delta(a_1 - a_2 - \mu) \delta(\sigma_1^2 + \sigma_2^2 - 2\rho\sigma_1\sigma_2 - \lambda^2), \quad (10)$$

where \mathcal{N} is a normalization constant, and $\delta(x)$ is the Dirac delta-function of distribution theory. That is, the prior distribution we will use in (6) is now the constrained

distribution $h_c(\mathbf{a}, \sigma)$, which represents the original assumptions concerning the distribution of \mathbf{a} and σ , i.e., $h(\mathbf{a}, \sigma)$, and the additional assumption that the mean and variance of the difference of the magnitudes are known.

In practice, the mean and variance of the difference of the magnitudes are not precisely known, and it may be more appropriate to treat these quantities as distributed. We will assume, however, that the no-yield data sets are sufficiently large such that using the delta-functions represents a reasonable approximation. This assumption allows us to explore the maximum benefit of using no-yield data.

The joint prior distribution $h(\mathbf{a}, \sigma)$ must still be specified. There are several joint prior distributions that are worth investigating. Shumway and Der [1990] consider a joint prior distribution that is the product of a bivariate normal for a given σ , and an inverted Wishart for σ . We will treat the a_i as joint normal random variates independent of σ_i and ρ , as is done by Nicholson et al. [1991]. That is, let

$$\begin{pmatrix} a_1 \\ a_2 \end{pmatrix} \sim N \left[\begin{pmatrix} \mu_{a_1} \\ \mu_{a_2} \end{pmatrix}, \begin{pmatrix} \sigma_{a_1}^2 & \rho_a \sigma_{a_1} \sigma_{a_2} \\ \rho_a \sigma_{a_1} \sigma_{a_2} & \sigma_{a_2}^2 \end{pmatrix} \right]. \quad (11)$$

Reasonable choices for the prior distribution of σ include the Wishart or inverted Wishart, which are multivariate sampling distributions, or if the σ_i and ρ are treated as independent random variables, one could use the product of independent sampling distributions (see, for example, Anderson [1958])

$$\frac{\sigma_i^2}{\sigma_{0i}^2} (N - 1) \sim \chi^2(N - 1) \quad (12)$$

$$\rho \sim \text{Approximately log normal.} \quad (13)$$

(The sampling distribution for ρ is rather cumbersome. An expression for this *pdf* may be found on p. 68 of Anderson [1958]). The parameters for this *pdf* are denoted by the mean, ρ_0 , and the number of degrees of freedom $N - 1$, which determines the variance. The parameters μ_{a_i} , σ_{a_i} , ρ_a , σ_{0i} , ρ_0 and N may be given by a panel of experts.

If the parameters of the joint prior are to be furnished by a panel, it is reasonable, and technically less tedious, to consider the case where the prior for σ is also given by a joint normal distribution, rather than the sampling distributions. This joint prior would reflect the panels ability to provide estimates of the *a priori* parameters and their uncertainties. Although it is certainly feasible to translate the

uncertainties furnished by a panel into an effective number of degrees of freedom, N , this choice of prior would alleviate the awkwardness of doing so. If this prior is used, it would be assumed that the means and variances of the normal distributions for σ_i and ρ are such that the probability that values of these random variables are outside of their physically acceptable ranges is effectively zero.

3.3 Summary of Technical Developments.

It is useful at this time to review our results to this point. We have shown that the unconstrained distribution of future magnitudes, given previous calibration data and prior information, may be given by

$$f(m_{1,n+1}, m_{2,n+1} | \vec{m}_n) = \int f_2(m_{1,n+1}, m_{2,n+1} | a, \sigma) f_3(a, \sigma | \vec{m}_n) da d\sigma, \quad (14)$$

where f_2 is given in (8),

$$f_3(a, \sigma | \vec{m}_n) = \frac{h(a, \sigma) L(\vec{m}_n | a, \sigma)}{\int h(a, \sigma) L(\vec{m}_n | a, \sigma) da d\sigma}, \quad (15)$$

$L(\vec{m}_n | a, \sigma)$ is given in (9), and $h(a, \sigma)$ is specified by (11)–(13).

Analogous expressions may also be given for the constrained distributions, which we denote with the subscript "c". Thus, the constrained distributions corresponding to f and f_3 are denoted by f_c and f_{3c} , and the constrained prior distribution is given by

$$h_c(a, \sigma) = \mathcal{N} h(a, \sigma) \delta(a_1 - a_2 - \mu) \delta(\sigma_1^2 + \sigma_2^2 - 2\rho\sigma_1\sigma_2 - \lambda^2), \quad (16)$$

where the normalization constant \mathcal{N} is needed to ensure that $h_c(a, \sigma)$ is a density normalized to unity.

We are almost in a position to develop a test of compliance. First, it is useful to define a weighted combination of the magnitudes by

$$m_{r,n+1} = r m_{1,n+1} + (1 - r) m_{2,n+1}, \quad (17)$$

where $0 < r < 1$. The marginal distribution of $m_{r,n+1}$, given \mathbf{a} and σ , is completely determined by the joint distribution f_2 of $m_{1,n+1}$ and $m_{2,n+1}$, given \mathbf{a} and σ . If we define this marginal distribution by $g_2(m_{r,n+1}|\mathbf{a}, \sigma)$, it is straightforward to show, using (8), that

$$g_2(m_{r,n+1}|\mathbf{a}, \sigma) = \frac{1}{\sqrt{2\pi}\sigma_r} \exp \left[-\frac{1}{2} \left(\frac{m_{r,n+1} - ra_1 - (1-r)a_2 - W_{n+1}}{\sigma_r} \right)^2 \right], \quad (18)$$

where $\sigma_r^2 = r^2\sigma_1^2 + (1-r)^2\sigma_2^2 + 2r(1-r)\rho\sigma_1\sigma_2$. If we also define $g(m_{r,n+1}|\vec{m}_n)$ to be the marginal distribution corresponding to the joint distribution $f(m_{1,n+1}, m_{2,n+1}|\vec{m}_n)$, then

$$g(m_{r,n+1}|\vec{m}_n) = \int da d\sigma g_2(m_{r,n+1}|\mathbf{a}, \sigma) f_3(\mathbf{a}, \sigma|\vec{m}_n). \quad (19)$$

There is an analogous expression, g_c , for the constrained marginal distribution. These are the distributions that will be used to test compliance.

SECTION 4

YIELD ESTIMATION AND TESTING COMPLIANCE

For $B_1 = B_2 = 1$, the log yield may be estimated in terms of the new weighted magnitude $m_{r,n+1}$ by

$$\hat{W}_{n+1} = m_{r,n+1} - r\hat{A}_1 - (1-r)\hat{A}_2 \quad (20)$$

where \hat{A}_1, \hat{A}_2 are estimates of the intercepts. For data only, \hat{A}_1, \hat{A}_2 may be taken to be the usual point estimates. Using prior information only, we can take $\hat{A}_1 = \mu_{a_1}$ and $\hat{A}_2 = \mu_{a_2}$. When data and prior information are available, the posterior means of a_1, a_2 are the most natural estimates of the intercepts. The posterior means may be computed as expectation values of a_1, a_2 using $f_{3c}(a, \sigma | \vec{m}_n)$.

We will establish a test of hypothesis based on the magnitude $m_{r,n+1}$, and compute the power and F-number of the test. The power of the test is the probability of rejecting the hypothesis that the true yield is in compliance with the treaty threshold. Note that basing the test on the magnitude is equivalent to basing the test on the AFTAC estimator of the log yield, which is given by (20), using constant panel estimates μ_{a_1} and μ_{a_2} for the unknown intercepts. The critical value of the test (defined below) in terms of this estimator is shifted by the constant $r\mu_{a_1} + (1-r)\mu_{a_2}$ relative to the critical value of the test in terms of the magnitude. The test is of course unchanged by this constant shift.

Alternatively, an estimate of the log yield, given in terms of the new magnitude and the posterior means of a_1 and a_2 , could be used in principle to establish a test of hypothesis. It is not clear whether this test is significantly different or better than the test in terms of the magnitude. This test is complicated, however, by the fact that the distribution of \hat{W}_{n+1} , in this case, is unknown. Shumway and Der [1990] encounter this obstacle in their analysis as well. Assuming unknown slopes in their work further complicates this matter. Rather than establishing a test of hypothesis in terms of the estimate of the log yield, they chose to compute confidence intervals for the new yield considered as a true fixed future observation.

Consider now a $100\alpha\%$ significance level test of the null hypothesis, $H_0 : W \leq W_T$, versus the alternative, $H_1 : W > W_T$, of the form:

$$\text{Reject } H_0 \text{ if } m_{r,n+1} > T_\alpha, \quad (21)$$

where W_T is the treaty threshold of the log yield, and T_α satisfies

$$P[m_{r,n+1} > T_\alpha | \vec{m}_n, W_{n+1} = W_T] = \alpha. \quad (22)$$

That is, assuming the true yield is at the treaty threshold, the critical value, T_α , is determined such that the hypothesis H_0 is falsely rejected only $100\alpha\%$ of the time. Using (19), (22) is equivalent to

$$\int_{T_\alpha}^{\infty} dm_{r,n+1} g(m_{r,n+1} | \vec{m}_n, W_{n+1} = W_T) = \alpha. \quad (23)$$

Once T_α is determined, the power of the test is defined to be the probability that the null hypothesis is rejected, i.e., for fixed T_α , the power at $W_{n+1} = W_0$ is given by

$$\text{Power}(W_0) = P[m_{r,n+1} > T_\alpha | \vec{m}_n, W_{n+1} = W_0]. \quad (24)$$

The F-number of the test is related to the power. Using the definition given by Alewine et al. [1988], the F-number is given by

$$F = 10^{W_F - W_T}, \quad (25)$$

where W_F is the value of the true log yield at which the power is 0.5. That is, W_F satisfies the equation

$$P[m_{r,n+1} > T_\alpha | \vec{m}_n, W_{n+1} = W_F] = 0.5. \quad (26)$$

It is important to understand that the power functions, computed in this way, represent the probabilities that the null hypothesis (i.e., the hypothesis that the yield of the event was in compliance with the treaty threshold) is rejected, only if the underlying assumptions are valid. That is, the expression in (24) is the true probability of calling a violation only if the weighted magnitude of the new event is distributed as in (19) for the unconstrained case, or analogously for the constrained case. Thus, for example, it is assumed that the intercepts are distributed as in (15). This expression

for the unconstrained case, and the analogous one for the constrained case, depend on the *a priori* assumptions. For practical monitoring applications these assumptions may not hold, however, they reflect our best estimation of the unknown calibration parameters based on *a priori* information, calibration data and no-yield data (in the constrained approach). As a result, the actual false alarm rate for monitoring a particular site may differ from the target value of α . We investigate this issue in more detail in Section 6.

SECTION 5

POWER COMPARISON

In order to assess the impact of imposing the prior information, particularly the constraints, it is useful to compare the power of the test for the constrained and unconstrained distributions. We will consider a special case of the formulation above, by treating the covariance matrix associated with the random errors as known, without uncertainty, so that analytic expressions may be obtained for the power and F-number. Nicholson et al. [1991] also make this assumption in their analysis. (A numerical simulation is needed to compute the power for the general case. Details of the simulation will be contained in a future report.) Consider the following four $100\alpha\%$ significance level tests:

- test 1 = a test of hypothesis based on the assumption that the calibration parameters (intercepts, slopes and covariance matrix) are completely known. In practice, this test is infeasible, however, it serves as a reference of the maximum possible power for fixed false alarm rate.
- test 2 = a test of hypothesis based on the constrained Bayesian approach, treating only the intercepts as unknown. (The only constraint used for this study is the one on the mean of the difference of the magnitudes.)
- test 3 = a test of hypothesis based on the unconstrained Bayesian approach, treating only the intercepts as unknown.
- test 4 = a test of hypothesis based on calibration data only, treating only the intercepts as unknown.

Tests 1-4, of the form (21), may be established by determining the distributions of $m_{r,n+1}$ under the appropriate assumptions. The expressions for the power, as computed in the previous section, and in more detail below, are the probabilities of detecting a violation for fixed false alarm rate, when the assumptions corresponding to each of the tests are valid. Thus, they represent the optimum power of each test.

For simplicity, and since the covariance matrix is assumed to be known, let $\rho = \rho(\epsilon_1, \epsilon_2)$, $\sigma_1 = \sigma_{\epsilon_1}$ and $\sigma_2 = \sigma_{\epsilon_2}$. To establish test 1, note that

$$\frac{m_{r,n+1} - W_{n+1} - A_r}{\sigma_r} \sim N(0, 1), \quad (27)$$

where $A_r \equiv rA_1 + (1-r)A_2$ and $\sigma_r^2 \equiv r^2\sigma_1^2 + (1-r)^2\sigma_2^2 + 2r(1-r)\rho\sigma_1\sigma_2$. (Cf. Alewine et al. [1988] and Gray and Woodward [1990]). To establish test 4 (previously considered by Hafemeister [1987]), we first define the usual point estimate of A_r by

$$\hat{A}_r = \frac{1}{n} \sum_{k=1}^n [rm_{1k} + (1-r)m_{2k} - W_k]. \quad (28)$$

It may then be shown that

$$\frac{m_{r,n+1} - W_{n+1} - \hat{A}_r}{\left(1 + \frac{1}{n}\right)^{1/2} \sigma_r} \sim N(0, 1). \quad (29)$$

The distributions of $m_{r,n+1}|\bar{m}_n$ for tests 2 and 3 may be computed using (8)–(11), (15) and (18) in (19), where Σ is now treated as a fixed matrix of known constants. Making these insertions, it is straightforward to show that for the constrained case

$$\frac{m_{r,n+1} - W_{n+1} - A_c}{\sqrt{\sigma_r^2 + \sigma_c^2}} \sim N(0, 1), \quad (30)$$

while for the unconstrained case

$$\frac{m_{r,n+1} - W_{n+1} - A_u}{\sqrt{\sigma_r^2 + \sigma_u^2}} \sim N(0, 1), \quad (31)$$

where

$$\sigma_c^2 = [\mathbf{u}'(\Sigma_a^{-1} + n\Sigma^{-1})\mathbf{u}]^{-1} \quad (32)$$

$$\sigma_u^2 = \frac{\mathbf{r}'_1(\Sigma_a^{-1} + n\Sigma^{-1})\mathbf{r}_1}{\det(\Sigma_a^{-1} + n\Sigma^{-1})} \quad (33)$$

$$A_c = \mathbf{r}'\boldsymbol{\mu}_a + \frac{n(\bar{\mathbf{X}} - \boldsymbol{\mu}_a)'\Sigma^{-1}\mathbf{u}}{\mathbf{u}'(\Sigma_a^{-1} + n\Sigma^{-1})\mathbf{u}} \quad (34)$$

$$A_u = \mathbf{r}'\boldsymbol{\mu}_a + \mathbf{r}'(\Sigma_a^{-1} + n\Sigma^{-1})^{-1} n\Sigma^{-1}(\bar{\mathbf{X}} - \boldsymbol{\mu}_a). \quad (35)$$

In these expression, we have defined the vectors $\mathbf{u}' = (1, 1)$, $\mathbf{r}' = (r, 1 - r)$, $\mathbf{r}_\perp' = (1 - r, -r)$, $\bar{\mathbf{X}}' = (\bar{m}_1 - \bar{W}, \bar{m}_2 - \bar{W})$, $\boldsymbol{\mu}'_a = (\mu_{a1}, \mu_{a2})$, where the prime is used to denote the transpose of a column vector. We have also defined

$$\Sigma = \begin{pmatrix} \sigma_1^2 & \rho\sigma_1\sigma_2 \\ \rho\sigma_1\sigma_2 & \sigma_2^2 \end{pmatrix} \quad (36)$$

$$\Sigma_a = \begin{pmatrix} \sigma_{a1}^2 & \rho_a\sigma_{a1}\sigma_{a2} \\ \rho_a\sigma_{a1}\sigma_{a2} & \sigma_{a2}^2 \end{pmatrix}, \quad (37)$$

and Σ^{-1} and Σ_a^{-1} denote their matrix inverses.

Using the distributions of (27) and (29)–(31), the critical values of the four tests may be obtained as in (23) such that the area under the distributions, to the right of the critical value, is α . The resulting critical values of the tests are

$$\begin{aligned} T_{1\alpha} &= Z_\alpha\sigma_r + W_T + A_r \\ T_{2\alpha} &= Z_\alpha\sqrt{\sigma_r^2 + \sigma_c^2} + W_T + A_c \\ T_{3\alpha} &= Z_\alpha\sqrt{\sigma_r^2 + \sigma_u^2} + W_T + A_u \\ T_{4\alpha} &= Z_\alpha\sigma_r\sqrt{1 + 1/n} + W_T + \hat{A}_r, \end{aligned} \quad (38)$$

where Z_α is the $100(1 - \alpha)$ percentile of $N(0, 1)$.

The power functions of the tests, at log yield W_0 , when the appropriate assumptions are correct, are given by

$$\begin{aligned}
\text{POWER}(W_0)_1 &= \text{erfc}(Z_\alpha + (W_T - W_0)/\sigma_r) \\
\text{POWER}(W_0)_2 &= \text{erfc}\left(Z_\alpha + (W_T - W_0)/\sqrt{\sigma_r^2 + \sigma_c^2}\right) \\
\text{POWER}(W_0)_3 &= \text{erfc}\left(Z_\alpha + (W_T - W_0)/\sqrt{\sigma_r^2 + \sigma_u^2}\right) \\
\text{POWER}(W_0)_4 &= \text{erfc}\left(Z_\alpha + (W_T - W_0)/\sigma_r\sqrt{1 + 1/n}\right),
\end{aligned} \tag{39}$$

where $\text{erfc}(x)$ is the complementary error function given by

$$\text{erfc}(x) = \frac{1}{\sqrt{2\pi}} \int_x^\infty e^{-z^2/2} dz. \tag{40}$$

It may also be shown that the F-numbers of the tests are given by

$$\begin{aligned}
F_1 &= 10^{Z_\alpha \sigma_r} \\
F_2 &= 10^{Z_\alpha \sqrt{\sigma_r^2 + \sigma_c^2}} \\
F_3 &= 10^{Z_\alpha \sqrt{\sigma_r^2 + \sigma_u^2}} \\
F_4 &= 10^{Z_\alpha \sigma_r \sqrt{1 + 1/n}}.
\end{aligned} \tag{41}$$

Note that although the critical values for tests 2, 3 and 4 depend on the calibration data, the power functions and F-numbers depend only on the sample size n , and not on the particular sample. Also, it is straightforward to show that if either $n \rightarrow \infty$ or $\sigma_{a_1}, \sigma_{a_2} \rightarrow 0$, then $\sigma_c, \sigma_u \rightarrow 0$.

Since these formulas are somewhat unwieldy, we have computed the power curves and F-numbers of the four tests for the cases listed in Table 1. We have set $\alpha = 0.025$ and $W_T = \log 150$. Figures 1-8 show the resulting power of the four tests as functions of the true yield, denoted by solid, dashed, dotted and dashed-dotted curves, respectively. The four frames in each figure show the results for $n = 0, 1, 2, 3$. The power curves of test 4 may be computed only for non-zero values of n . The

Table 1. List of parametric cases for the power comparison.

Case	σ_1	σ_2	ρ	σ_{a_1}	σ_{a_2}	ρ_a
1	0.05	0.05	0.5	0.05	0.05	0.0
2	0.05	0.05	0.5	0.05	0.05	0.5
3	0.05	0.05	0.5	0.05	0.10	0.0
4	0.05	0.05	0.5	0.05	0.10	0.5
5	0.05	0.10	0.5	0.05	0.05	0.0
6	0.05	0.10	0.5	0.05	0.05	0.5
7	0.05	0.10	0.5	0.05	0.10	0.0
8	0.05	0.10	0.5	0.05	0.10	0.5

corresponding F-numbers are given in the legends. Note that in Figures 1, 2, 5 and 6, the power curves of tests 2 and 3 are identical.

There are several significant points to make concerning these results:

1. Test 1 is clearly the test with the greatest power in all cases. This is expected since there is no uncertainty in the calibration parameters.
2. The power of test 2 is greater than or equal to the power of test 3 and, hence, the F-numbers of test 2 are less than or equal to those of test 3 in all cases.
3. Equality occurs for cases in which the standard deviations of the random errors and intercepts are the same for both magnitudes (e.g., Figures 1, 2 for all values of n and Figures 5, 6 for $n = 0$.) Note that for $n = 0$, the random errors contribute identically to the power of tests 2 and 3 via σ_r^2 . For $n > 0$, Figures 5 and 6 show that the power of test 2 is slightly greater than that of test 3 even though the uncertainty in the intercepts is the same for both magnitudes.
4. The greatest increase in power of test 2 relative to test 3 occurs when the uncertainty in one of the intercepts is much larger than the other (e.g., Figures 3, 4, 7, 8). Note that for $n > 0$ the power of test 3 rapidly converges to that of test 2 for the cases shown in Figures 3 and 4. Figures 7 and 8 show that the convergence is slower for cases in which $\sigma_2 > \sigma_1$.
5. In all cases, the power curves of tests 2, 3 and 4 converge to the power curve of test 1 as n increases.

6. In all cases, test 4 (based only on calibration data) has the least power of the four tests.

These results show that the optimum power of the constrained test is always at least as great as that of the unconstrained test. The constraint, based on the no-yield data, provides the greatest benefit for cases in which there is greater uncertainty in one of the intercepts. It is not surprising that for equivalent *a priori* assumptions regarding the uncertainty in the intercepts, the constrained and unconstrained tests provided similar results. The power computed for test 2 assumes that a constraint physically exists and makes use of that information to compute the critical value of the test. Alternatively, the power computed for test 3 assumes that the difference in the intercepts is not necessarily a fixed constant and, hence, ignores this information when computing the critical value of the test. Thus, the power functions of tests 2 and 3 represent the optimum power of each test, but they are being compared for two physically different situations.

A useful comparison of tests 2 and 3 would be to assume that the magnitudes, are distributed as assumed in the constrained case, but only the constrained approach makes use of that information to set the critical value. This comparison is more realistic since, in practice, the difference in the intercepts and hence the difference in the expected magnitudes are given by a fixed constant. The constrained approach makes use of the no-yield data to determine what this fixed constant is, while the unconstrained approach does not.

Rather than perform this comparison, for which the Bayesian assumptions would still differ from the assumptions of test 1, we will examine the case in which the magnitudes are distributed as assumed in tests 1 and 4, i.e., as in (1), but the critical values of each test are set as above. The actual probabilities of calling a violation based on each of the four tests may then be compared under the same test site conditions. This comparison is contained in the following section.

SECTION 6

ROBUSTNESS

An important issue regarding the monitoring of a particular test site is the robustness of the test of compliance to the assumptions that are made in the statistical methodology. In particular, the test of compliance, based on a Bayesian approach, depends on the assumed parameters of the prior distribution. It is important to note that the expression for the power in (24), and the power of the Bayesian tests computed in the previous section are the true probabilities of calling violations only if the magnitudes of the new events are distributed as in (19) for the unconstrained case, or the analogous expression for the constrained case. The expressions, however, are only estimates of the true distribution which depends on the true, but unknown, intercept, slope and covariance matrix parameters.

An alternative interpretation of the power of the Bayesian tests is the following. Consider the case where $n = 0$. Then the power computed above is the true probability of calling a violation only if the assumed prior is correct, i.e., only if the intercepts are actually distributed as assumed in the constrained or unconstrained priors. In this sense, the joint priors may be interpreted as distributions of all possible test sites. For a particular test site, however, the intercepts are not distributed. Rather, they have fixed, although unknown values. Thus, the false alarm rate using a Bayesian approach, for a sequence of events at a particular test site, is not necessarily α . We refer to the false alarm rate, power and F-number in this case as the "actual" quantities, "conditional" on the values of the intercepts for the given test site.

Here we assess the robustness of the actual power of the tests based on the Bayesian approaches. That is, suppose we set the critical value T_α as before. We now want to determine the actual power of the test, conditional on the true values of the intercepts, $A' = (A_1, A_2)$, when the means of the Bayesian prior are not necessarily equal to them, e.g., we will consider cases in which

$$\mu_{a_i} = A_i \pm c\sigma_{a_i}, \quad c = 0, \pm 1, \pm 2. \quad (42)$$

The conditional power is the probability that m_r is greater than the critical value, weighted over the distribution of all possible critical values. Thus,

$$\text{POWER}(W_0|\mathbf{A}) = \int dT_\alpha p[T_\alpha|\bar{m}_n, W = W_0] P[m_r > T_\alpha; \mathbf{A}, \Sigma|W = W_0], \quad (43)$$

where

$$P[m_r > T_\alpha; \mathbf{A}, \Sigma|W = W_0] = \frac{1}{\sqrt{2\pi}\sigma_r} \int_{T_\alpha}^{\infty} dm_r \exp \left[-\frac{1}{2} \left(\frac{m_{r,n+1} - A_r - W_{n+1}}{\sigma_r} \right)^2 \right]. \quad (44)$$

It may be shown that the actual power functions of tests 1 and 4 are the same as those computed in (39). The distributions of the critical values for tests 2 and 3 may be determined from (32)–(35) and (38). Also, since A_c and A_u depend linearly on the randomly distributed mean magnitudes \bar{m}_1 and \bar{m}_2 , it may be shown that, for tests 2 and 3, T_α is distributed as

$$\frac{T_\alpha - \mu_T}{\sigma_T} \sim N(0, 1), \quad (45)$$

where for the constrained case

$$\mu_{T_{2\alpha}} = E[T_{2\alpha}] = Z_\alpha \sqrt{\sigma_r^2 + \sigma_c^2} + W_T + A_r + \frac{(\mu_a - \mathbf{A})' \Sigma_a^{-1} \mathbf{u}}{\mathbf{u}'(\Sigma_a^{-1} + n\Sigma^{-1})\mathbf{u}} \quad (46)$$

$$\sigma_{T_{2\alpha}}^2 = \text{Var}[T_{2\alpha}] = \frac{n\mathbf{u}'\Sigma^{-1}\mathbf{u}}{[\mathbf{u}'(\Sigma_a^{-1} + n\Sigma^{-1})\mathbf{u}]^2}, \quad (47)$$

while for the unconstrained case

$$\mu_{T_{3\alpha}} = E[T_{3\alpha}] = Z_\alpha \sqrt{\sigma_r^2 + \sigma_u^2} + W_T + A_r + \mathbf{r}'(\Sigma_a^{-1} + n\Sigma^{-1})^{-1} \Sigma_a^{-1}(\mu_a - \mathbf{A}) \quad (48)$$

$$\sigma_{T_{3\alpha}}^2 = \text{Var}[T_{3\alpha}] = n\mathbf{r}'(\Sigma_a^{-1} + n\Sigma^{-1})^{-1} \Sigma^{-1}(\Sigma_a^{-1} + n\Sigma^{-1})^{-1} \mathbf{r} \quad (49)$$

In obtaining these expressions, it is assumed that the magnitudes are distributed as in (1), and $\mathbf{r}'\mathbf{A} = A_r$. Note that in the constrained case, $A_2 = A_1 - \mu$ and $\mu_{a_2} = \mu_{a_1} - \mu$,

hence, $(\mu_a - A)' = (\mu_{a_1} - A_1)u' = (\mu_{a_2} - A_2)u'$. This relationship does not hold for the unconstrained case.

Using (43)–(49), the actual power for tests 2 and 3, conditional on A , may be expressed as

$$\text{POWER}(W_0|A) = \text{erfc}(\zeta_\alpha), \quad (50)$$

where

$$\zeta_\alpha = \frac{\mu_T - A_r - W_0}{\sqrt{\sigma_r^2 + \sigma_T^2}}. \quad (51)$$

It is straightforward to show that as $n \rightarrow \infty$, $\mu_{T_{2a}}, \mu_{T_{3a}} \rightarrow Z_\alpha \sigma_r + W_T + A_r$ and $\sigma_{T_{2a}}^2, \sigma_{T_{3a}}^2 \rightarrow 0$. Thus, in the limit as $n \rightarrow \infty$, the power curves of tests 2 and 3 converge to that of test 1, and the false alarm rates of tests 2 and 3 approach α . It may also be shown that the same result occurs if $\mu_a = A$ and $\sigma_{a_1}, \sigma_{a_2} \rightarrow 0$.

To illustrate the results, we have plotted the actual power curves of the four tests as functions of the yield for the cases listed in Table 2. For each of these cases we have considered five combinations of the prior means of the intercepts listed in table 3.

Table 2. List of parametric cases for the conditional power comparison.

Case	σ_1	σ_2	ρ	σ_{a_1}	σ_{a_2}	ρ_a
1	0.05	0.05	0.5	0.05	0.05	0
2	0.05	0.05	0.5	0.05	0.10	0
3	0.05	0.05	0.5	0.05	0.15	0

Figures 9(a-e)–11(a-e) show the results for these cases. As before, the solid, dashed and dotted curves represent the power functions of tests 1, 2 and 3, respectively. The four frames in each figure show the results for $n = 0, 1, 2, 3$. The actual false alarm rates achieved by each of the tests are shown in the figure legends. The power curves of test 1 represent the maximum probability of detecting a violation, at a particular yield, for a fixed false alarm rate. This test is infeasible, however, the performance of

Table 3. List of prior means used for each of the cases listed in Table 2.

Case	$(\mu_{a_1} - A_1)/\sigma_{a_1}$	$(\mu_{a_2} - A_2)/\sigma_{a_2}$
a	0	0
b	0	2
c	0	-2
d	2	2
e	-2	-2

the other two tests should be measured by the similarity of the their power curves to those of test 1.

The significant results of this study are the following:

1. For all cases in which neither of the means of the prior were chosen to be two standard deviations less than the true intercepts, the power of test 2 is greater than or equal to that of test 3, i.e., except for those cases labelled by "c" and "e".
2. The cases for which the power of test 2 is dramatically better than that of test 3 are those in which $\mu_{a_2} = A_2 + 2\sigma_{a_2}$, particularly if $\mu_{a_1} = A_1$, but even if $\mu_{a_1} = A_1 + 2\sigma_{a_1}$. See, for example, Figures 9(b,d)-11(b,d). Also, cases in which σ_{a_2} is significantly greater than σ_{a_1} , lead to greater relative power of test 2 to test 3. Compare Figure 9, 10 and 11.
3. The power of tests 2 and 3 are equal if the $\sigma_{a_1} = \sigma_{a_2}$ and $\sigma_1 = \sigma_2$ (provided $n = 0$). See, for example, Figures 9a for all values of n and 12a for $n = 0$.
4. For those cases labelled by "c" and "e", in which one or both of the means of the prior were chosen to be two standard deviations less than the true intercepts, the power of test 3 is greater than that of test 2, but the false alarm rates of test 3 are also noticeably greater than 0.025. The false alarm rates of test 2 are greater than 0.025 only for the cases labelled by "e", but are still considerably smaller than the false alarm rates of test 3.
5. For the cases examined, the largest actual false alarm rate for test 2 was 0.084 (Figure 9e), while for test 3 the largest actual false alarm rate was 0.705. After as few as two calibration events the false alarm rate of test 2 was no greater than 0.055 for all of these cases.

6. The power of test 2 (constrained Bayesian) was less than that of the test 4 (calibration data only), except for cases in which both prior means of the intercepts were two standard deviations greater than the true intercepts.

These results show that the constrained Bayesian approach is far more robust than the unconstrained approach. That is, the power curves of test 2 (constrained Bayesian approach) are far less sensitive to uncertainties in the intercepts and incorrect assumptions regarding the prior means of the intercepts. It was much more likely that test 3 (unconstrained Bayesian approach) had dramatically less power or, alternatively, a false alarm rate that was dramatically too large. For all of the cases considered here, the power of test 2 was always closer to the target power of test 1 than the power of test 3.

Comparisons to test 4 show that the power of test 2 is greater in all cases, except those for which both prior means of the intercepts are considerably larger than the true values. The priors, however, are presumably assigned with sufficient confidence so that the probability of such an occurrence is extremely small ($< 2\%$). In contrast, if either or both of the prior means were two standard greater than the true intercepts, the power of test 3 was less than that of test 4.

The study just described was repeated for $\sigma_2 = 0.10$, with all of the other parameters in Tables 2 and 3 the same as before. The results are very similar to those presented in Figures 9-11. The relative improved performance of test 2 to test 3 was slightly more pronounced for these cases as it was for the power comparison in Section 5.

SECTION 7

CONCLUSIONS AND FUTURE WORK

In this report, we have developed a constrained Bayesian approach for estimating the yield for a future underground test based on expert prior information, calibration data (if available) and no-yield data. The approach was formulated for the case in which the intercepts and the covariance matrix of the random seismic errors are unknown.

The results of the power comparison in Section 5, treating only the intercepts as unknown, showed that the test of hypothesis based on the constrained Bayesian approach is always as good or better than the Bayesian test without the constraint, and is always better than the test based only on calibration data when the appropriate Bayesian assumptions hold. The constrained approach is particularly useful for cases in which the uncertainty in one of the intercepts is relatively large, and little or no calibration data is available.

The robustness study in Section 6 showed that the constraint, based on the no-yield data, greatly corrects for poor prior information regarding either or both intercepts. If the prior means of the intercepts are chosen too small, the false alarm rate of the constrained approach may exceed 0.025, but will be considerably closer to the desired value than the false alarm rate of the unconstrained approach. The actual power of the unconstrained test was greater in these cases, but this test is not favored because of the high false alarm rate. In all other cases, the actual power of the constrained test was at least as great as that of the unconstrained test.

If there is no calibration data, the constrained approach is the best of the methods explored here for testing TTBT compliance. If the experts are confident that both prior means of the intercepts have not been dramatically underestimated or overestimated, the power of the constrained approach, for significance level less than or equal to 0.025, is greater than the approach based only on calibration data, requiring roughly half as many calibration events to achieve the same F-number as the latter test.

In the future, a simulation should be performed to compare the power functions of tests similar to tests 2, 3 and 4 above, but also treating the covariance matrix of the random seismic errors as unknown, which indeed it is. This simulation is near completion, but we were unable to obtain the results in time for this report. The

importance of treating the covariance matrix as unknown is illustrated in Figures 12 and 13, which show the power curves of three tests for two different values of σ_2 . Tests 1 and 2 correspond to tests 1 and 4 above, i.e., treating all of the parameters as known for the first, and only the intercepts as known for the second. For test 3, the intercepts and the covariance matrix are treated as unknown, using only calibration data to estimate them. This test may be based on Student's t -distributions as shown by Alewine et al. [1988] and Gray and Woodward [1990].

These figures show that the treatment of the covariance matrix is very important. In many of the previous figures the power curves of all four tests were not dramatically different. However, for the realistic case in which the covariance matrix is treated as unknown, the differences in the tests are expected to be much more significant. For example, a test based on calibration data alone, and the assumption of unknown intercepts and covariance matrix, cannot be used unless data for at least two calibration events are available.

There is still considerable work that can be done to improve our approach. In the future, we will extend our analysis to treat the case of unknown slopes. This extension is important if this approach is to have monitoring applications relevant to a low-yield or comprehensive test ban treaty. We will also explore the effect of relaxing the assumption that μ and λ^2 are exactly known. This is a necessary modification in order to apply the constrained Bayesian approach to monitoring test sites for which there is limited no-yield data.

SECTION 8

REFERENCES

Alewine, R.W. III, H.L. Gray, G.D. McCartor and G.L. Wilson (1988). "Seismic Monitoring of a Threshold Test Ban Treaty (TTBT) Following Calibration of the Test Site with CORTEX Experiments", AFGL-TR-88-0055, Air Force Geophysics Laboratory, Hanscom AFB, Massachusetts 01731, ADB122971.

Anderson, T.W. (1958). *An Introduction to Multivariate Statistical Analysis*, John Wiley & Sons, New York.

Gray, H.L. and W.A. Woodward (1990). "Some Remarks on Compliance Testing", GL-TR-90-0282, Air Force Geophysics Laboratory, Hanscom AFB, Massachusetts 01731, ADA231936.

Hafemeister, D.W. (1987). Private communication.

Nicholson W.L., R.W. Mensing, and H.L. Gray (1991). Private communication.

Shumway, R.H. and Z.A. Der (1990). "Multivariate Calibration and Yield Estimation for Nuclear Tests", University of California, Davis.

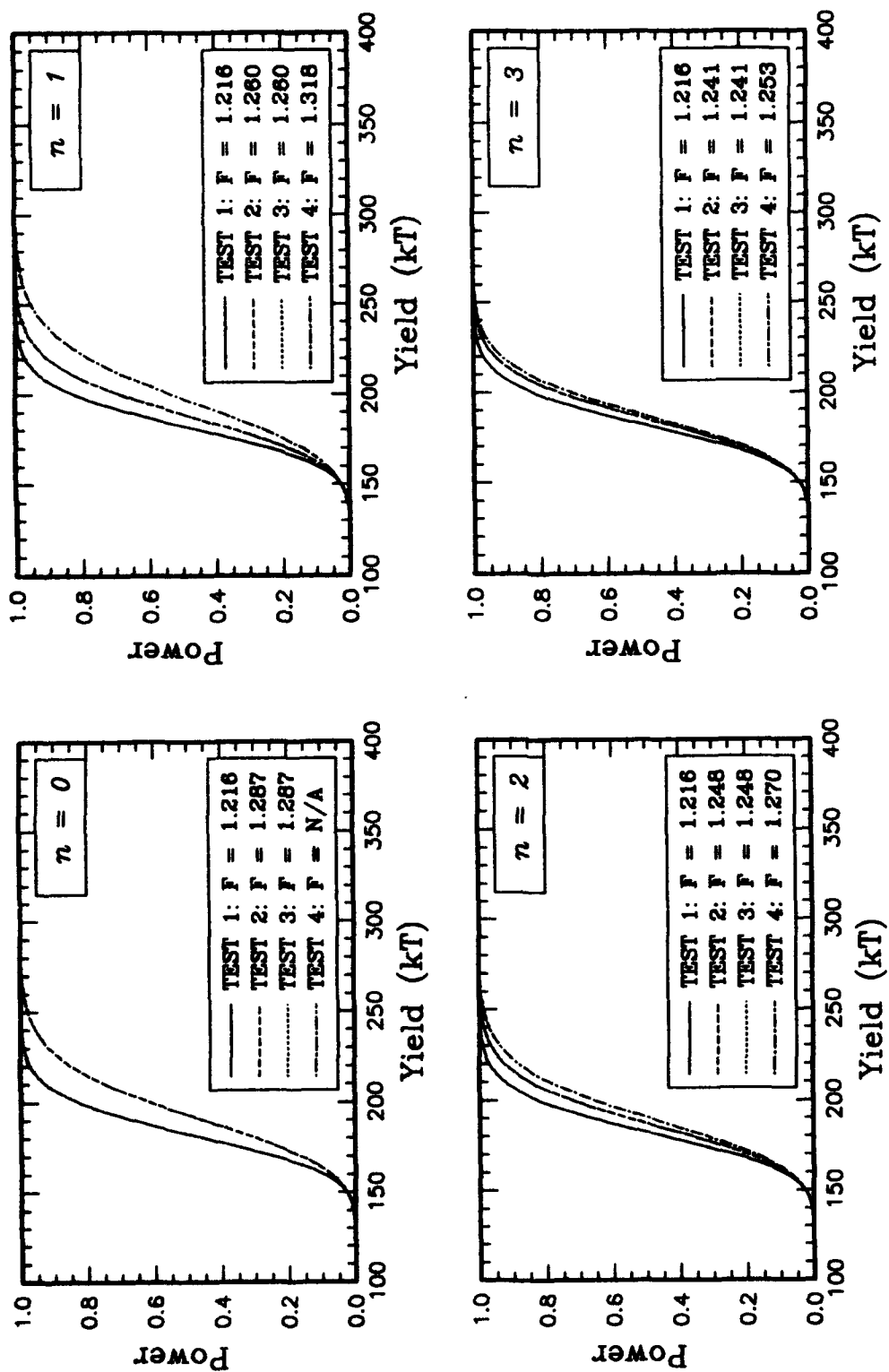


Figure 1. Power curves of the four tests as functions of yield for the case in which $\sigma_1 = .05, \sigma_2 = .05, \rho = .5, \sigma_{\omega} = .05, \sigma_{\epsilon} = .05, \rho_{\epsilon} = .0$.

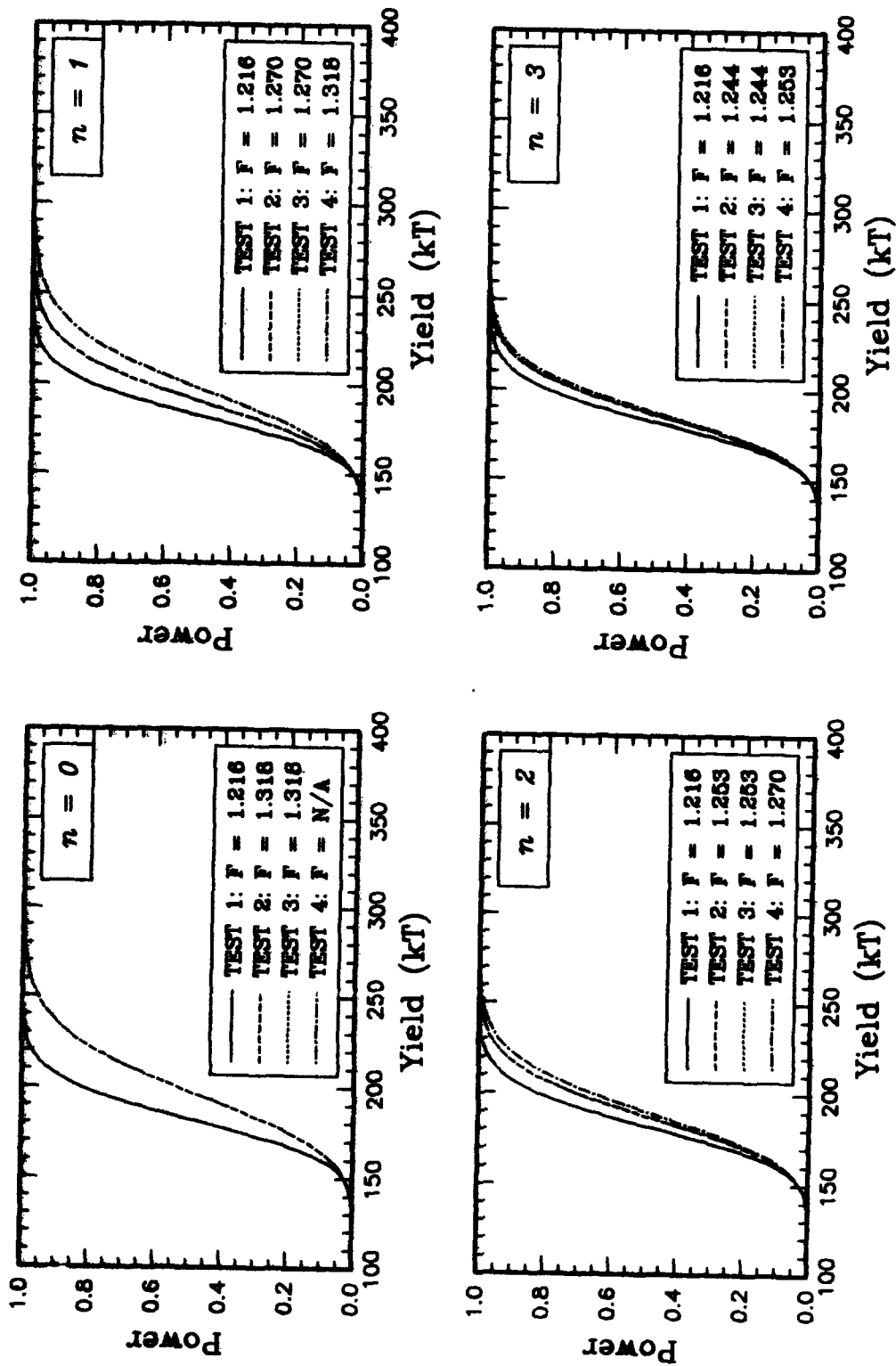


Figure 2. Power curves of the four tests as functions of yield for the case in which $\sigma_1 = .05$, $\sigma_2 = .05$, $\rho = .5$, $\sigma_w = .05$, $\sigma_e = .05$, $\rho_e = .5$.

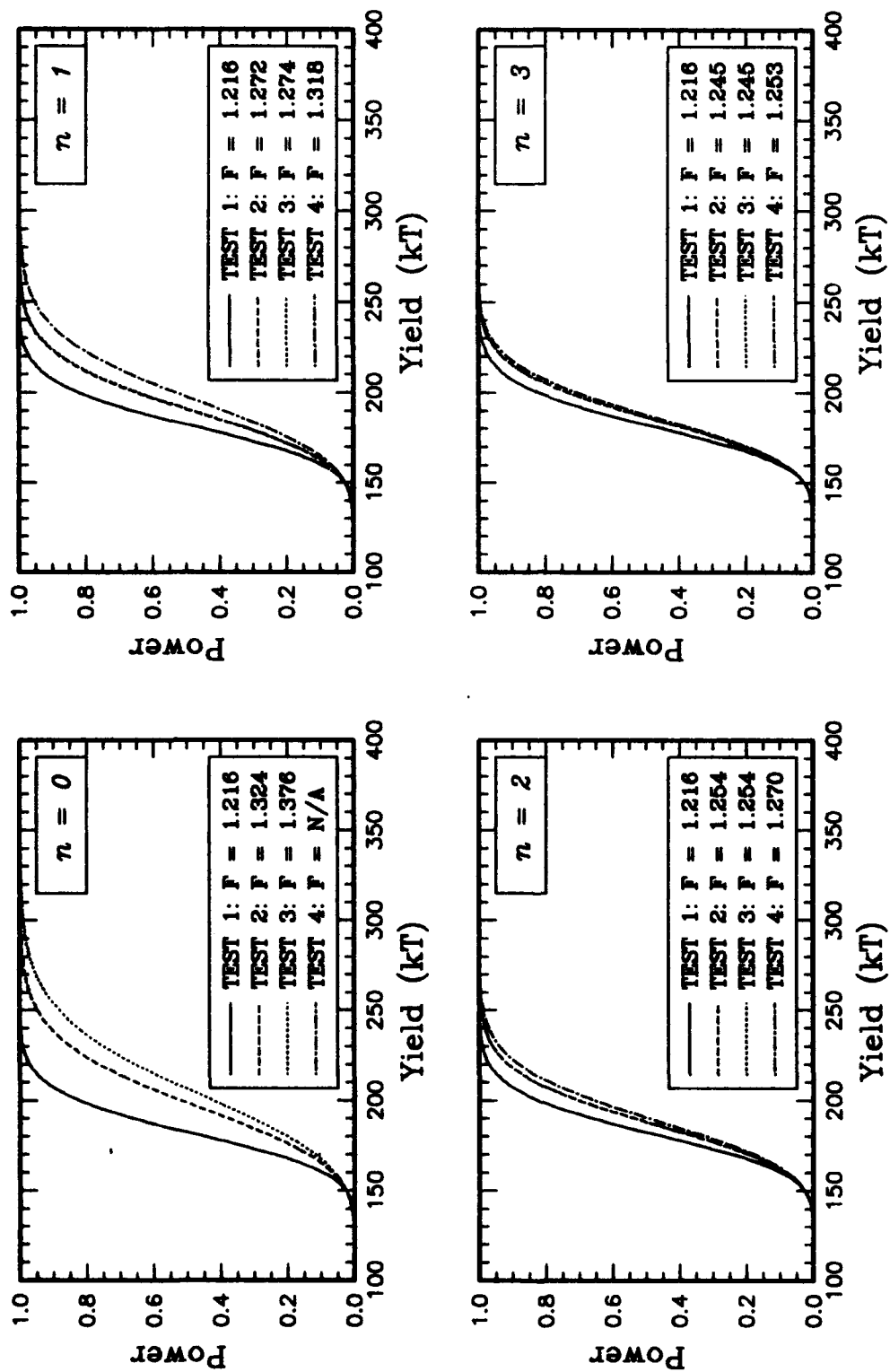


Figure 3. Power curves of the four tests as functions of yield for the case in which $\sigma_1 = .05$, $\sigma_2 = .05$, $\rho = .5$, $\sigma_w = .05$, $\sigma_d = .10$, $\rho_s = .0$.

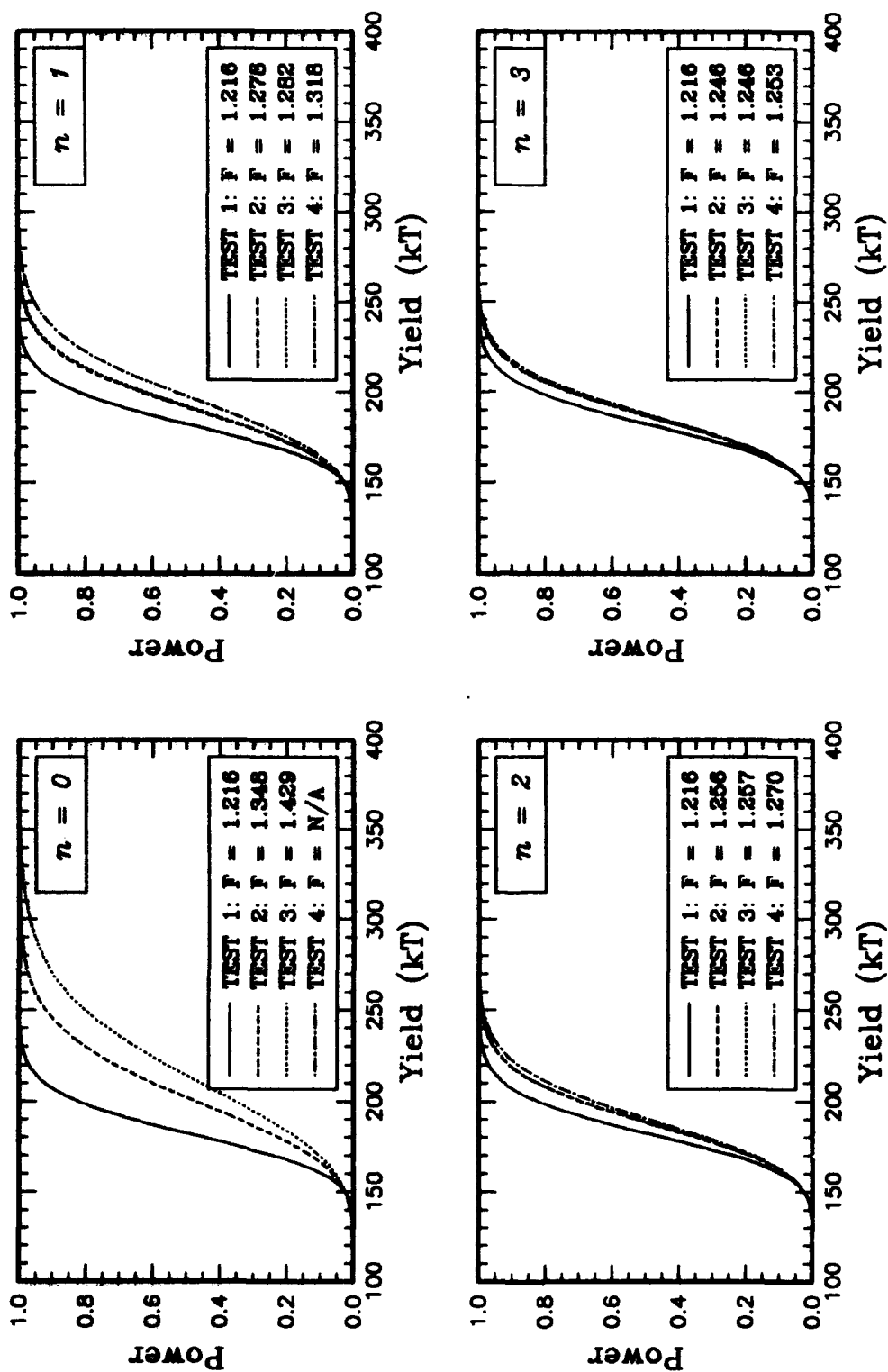


Figure 4. Power curves of the four tests as functions of yield for the case in which $\sigma_1 = .05$, $\sigma_2 = .05$, $\rho = .5$, $\sigma_{ad} = .05$, $\sigma_{ad} = .10$, $\rho_a = .5$.

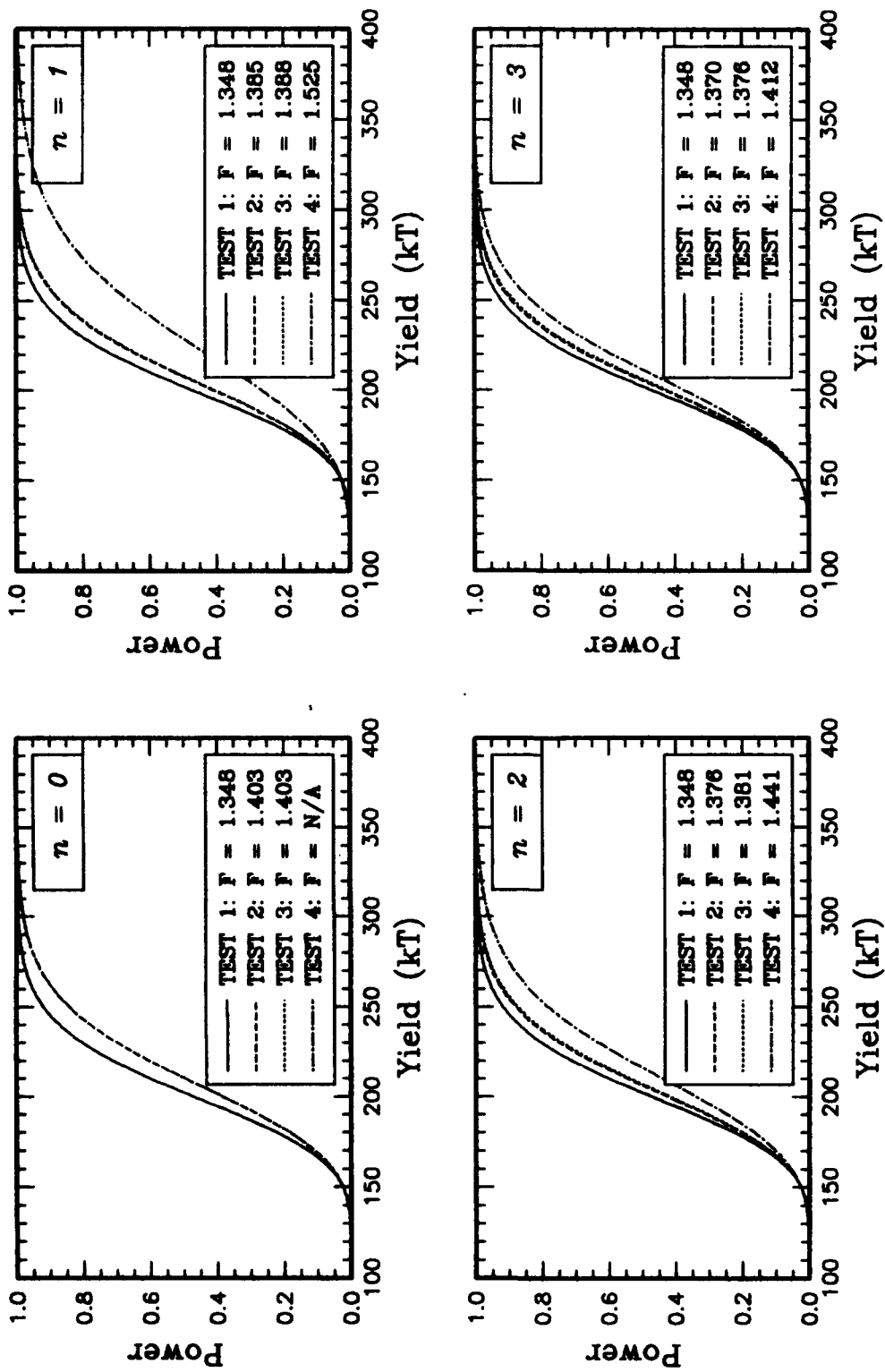


Figure 5. Power curves of the four tests as functions of yield for the case in which $\sigma_1 = .05$, $\sigma_2 = .10$, $\rho = .5$, $\sigma_d = .05$, $\sigma_a = .05$, $\rho_a = .0$.

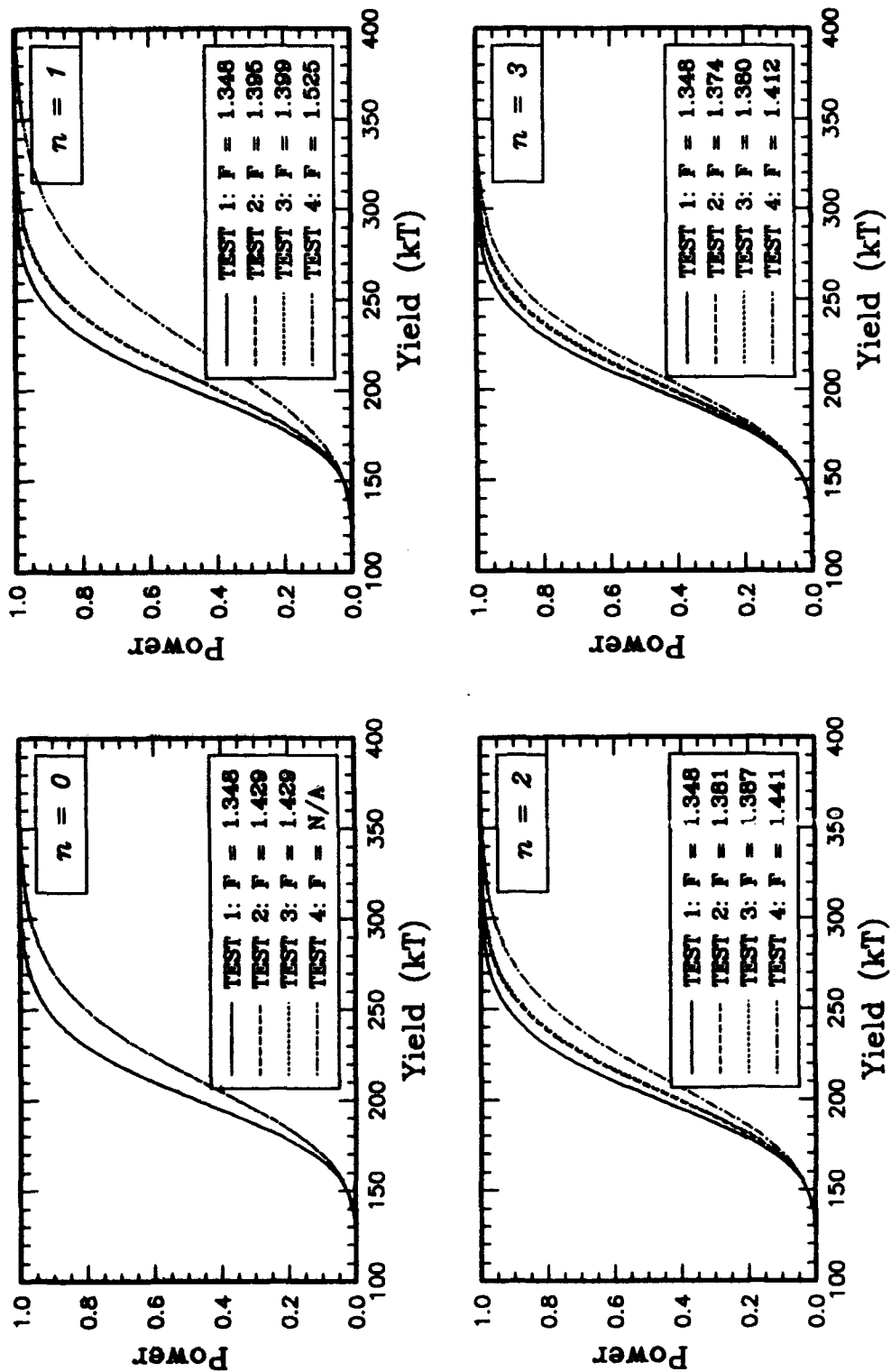


Figure 6. Power curves of the four tests as functions of yield for the case in which $\sigma_1 = .05$, $\sigma_2 = .10$, $\rho = .5$, $\sigma_d = .05$, $\sigma_e = .05$, $\rho_s = .5$.

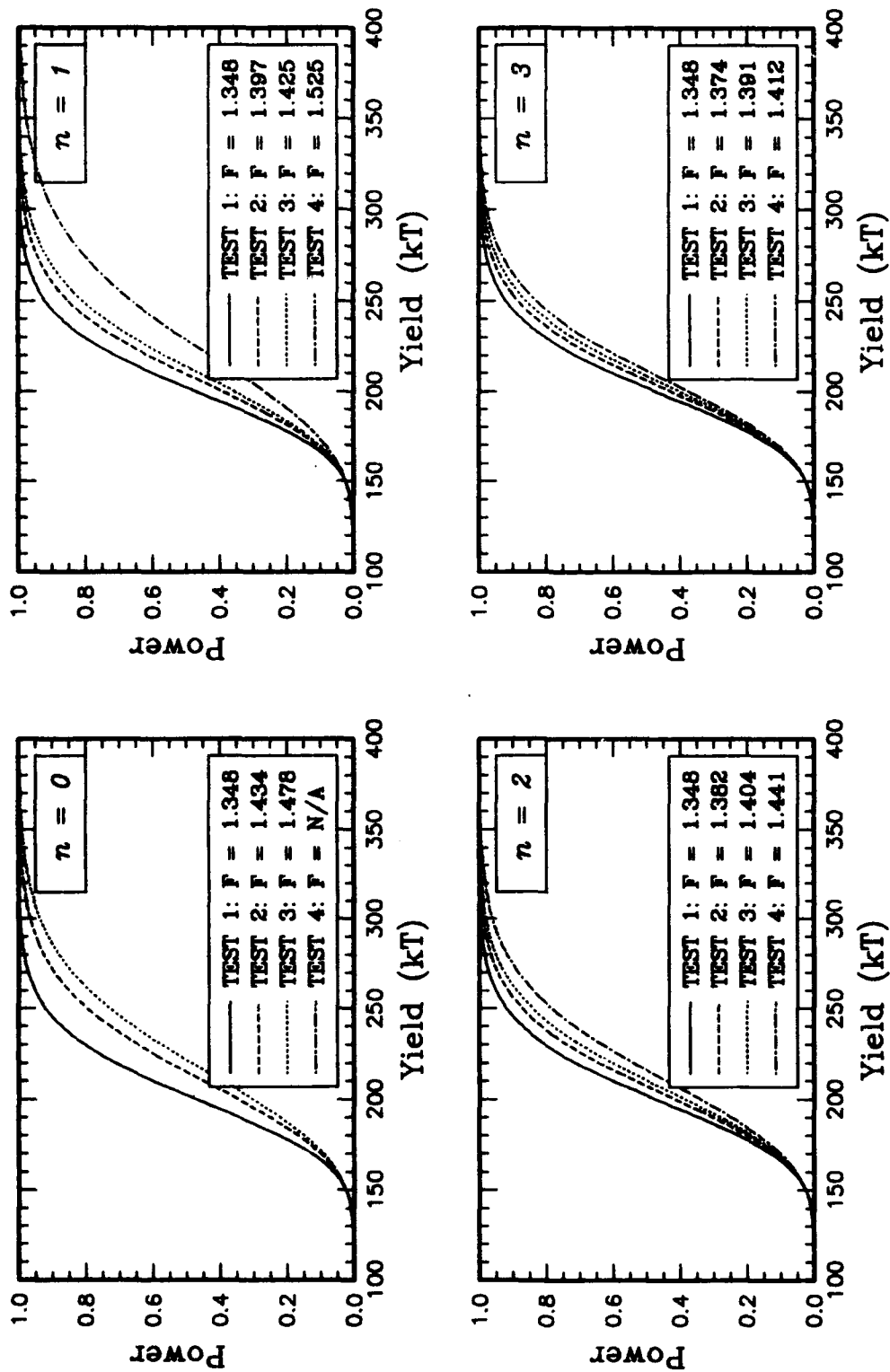


Figure 7. Power curves of the four tests as functions of yield for the case in which $\sigma_1 = .05$, $\sigma_2 = .10$, $\rho = .5$, $\sigma_M = .05$, $\sigma_{\Delta} = .10$, $\rho_{\Delta} = .0$.

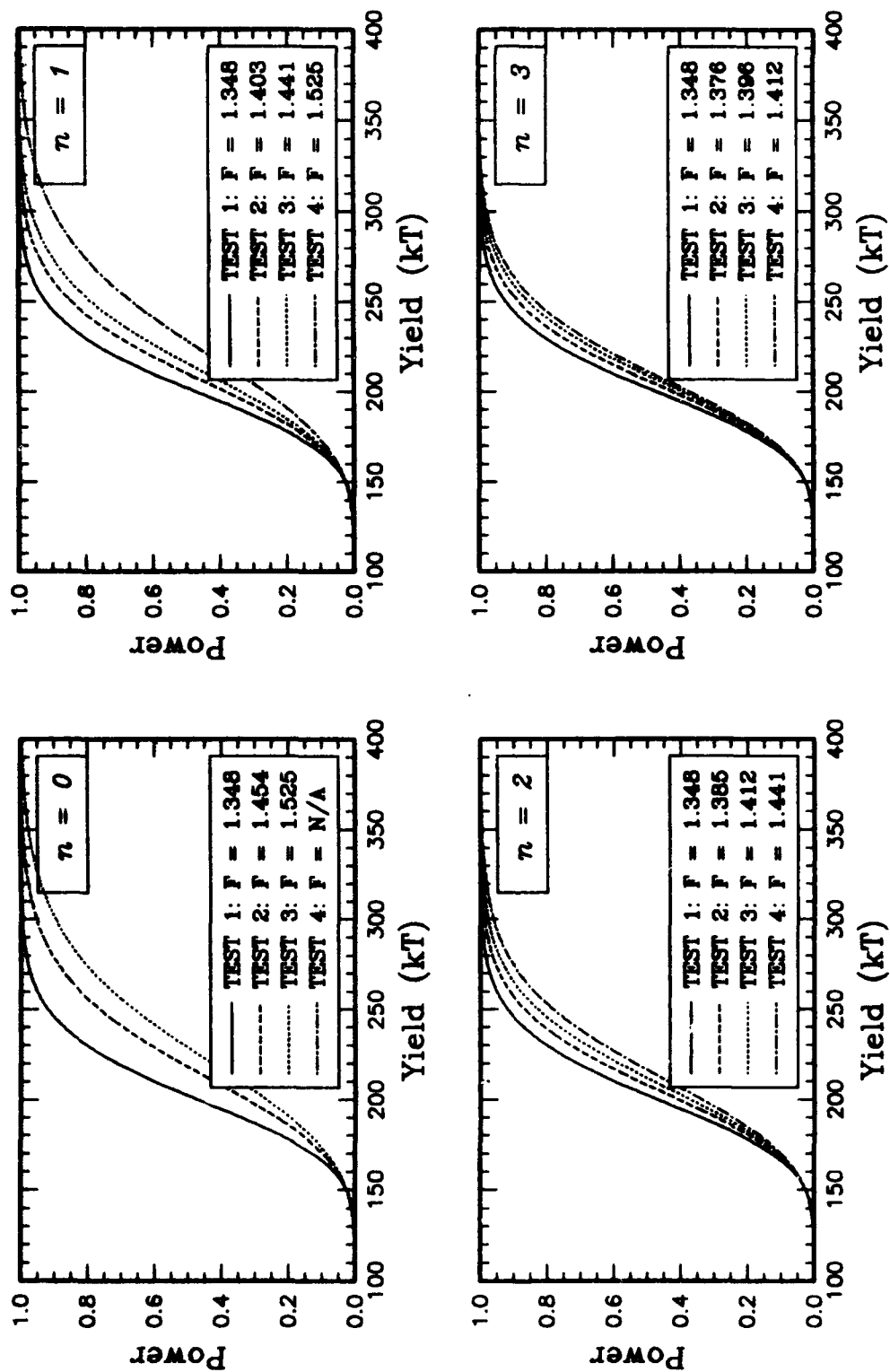


Figure 8. Power curves of the four tests as functions of yield for the case in which $\sigma_1 = .05$, $\sigma_s = .10$, $\rho = .5$, $\sigma_w = .05$, $\sigma_a = .10$, $\rho_a = .5$.

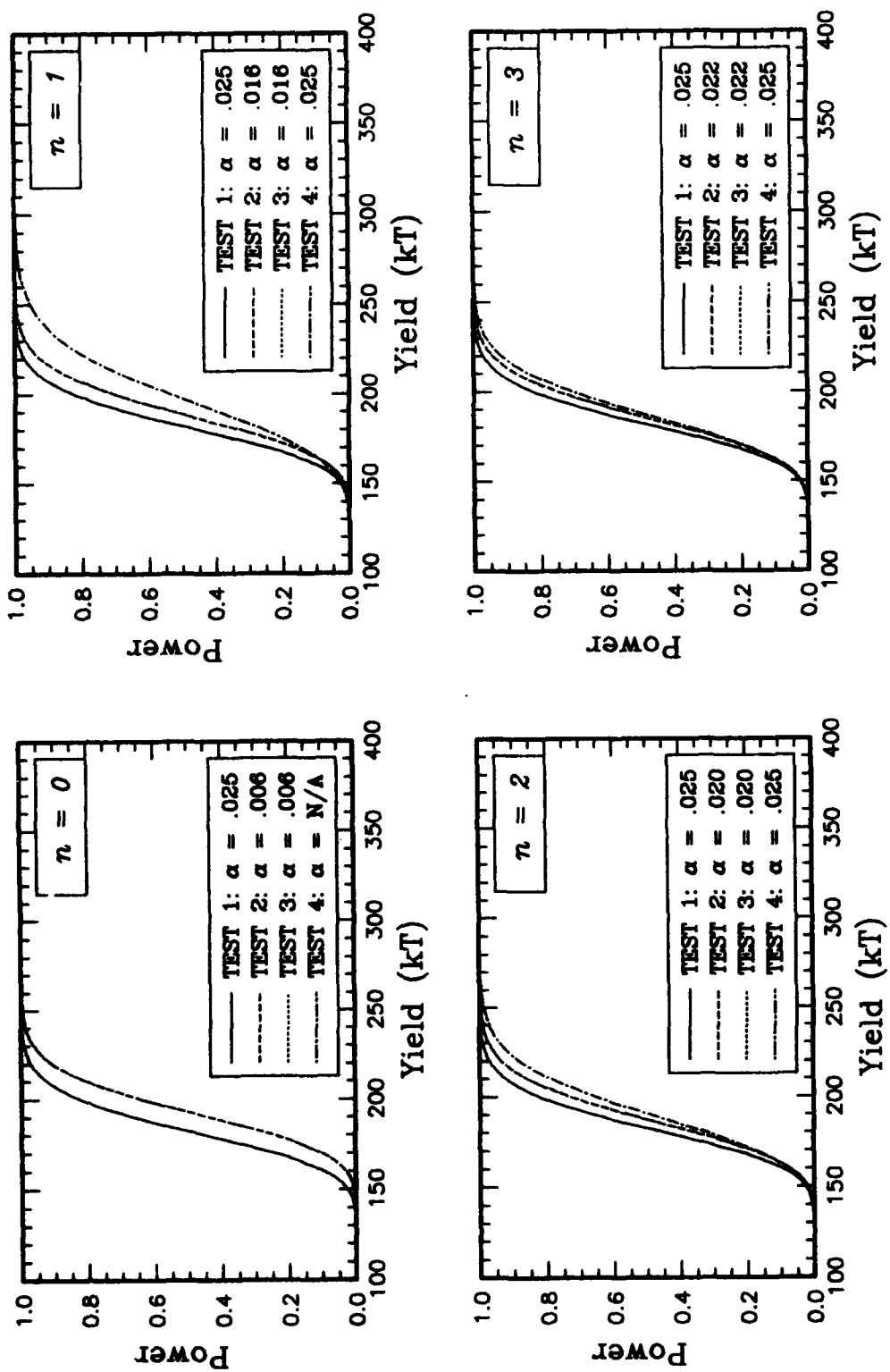


Figure 9a. Actual power curves of the four tests, as functions of yield, for the case in which $\sigma_1 = .05$, $\sigma_2 = .05$, $\rho = .5$, $\sigma_{\sigma'} = .05$, $\sigma_{\sigma} = .05$, $\rho_{\sigma} = .0$, and $(\mu_{\sigma} - A_1)/\sigma_{\sigma'} = 0$, $(\mu_{\sigma} - A_2)/\sigma_{\sigma} = 0$.

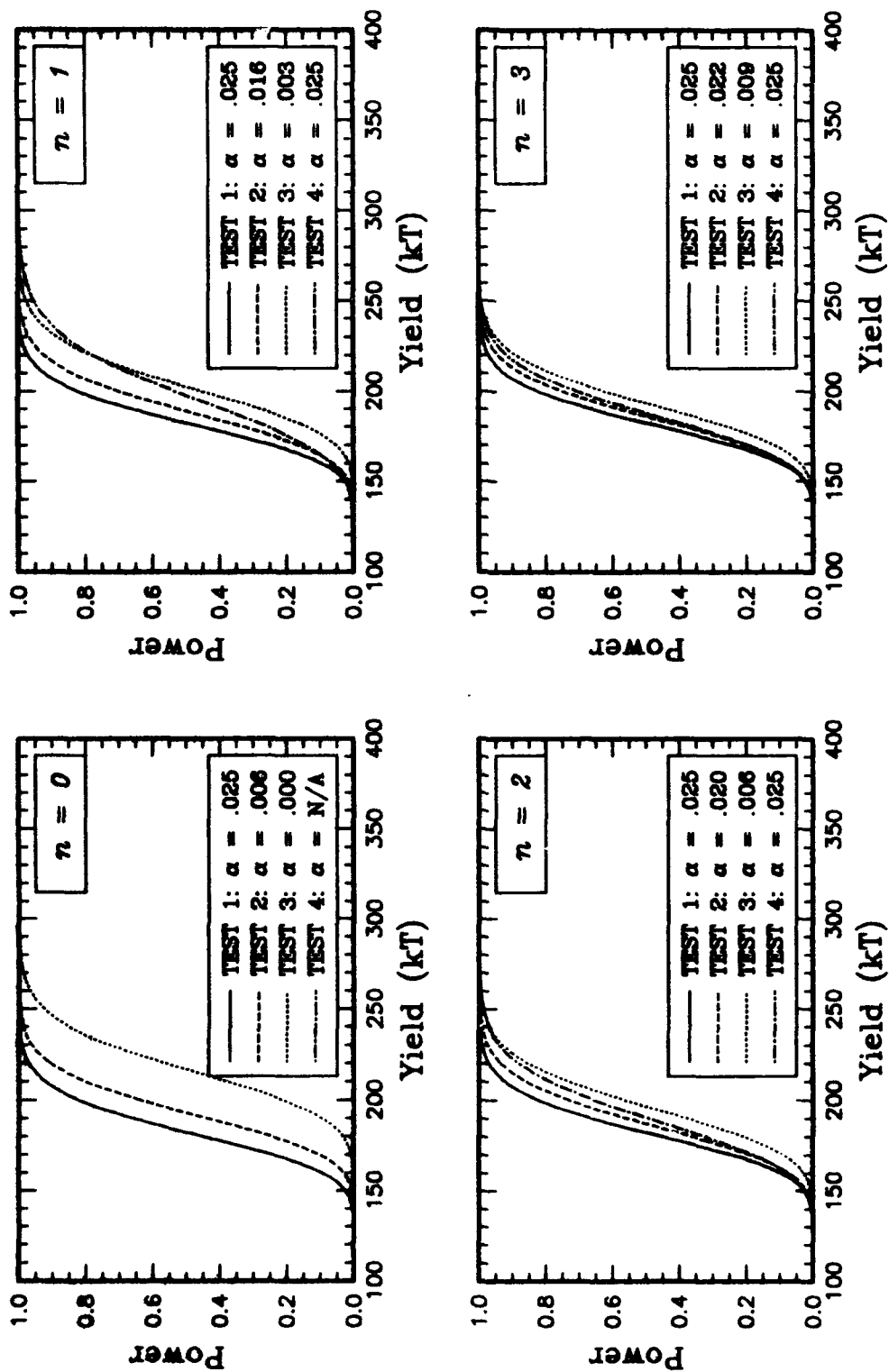


Figure 9b. Actual power curves of the four tests, as functions of yield, for the case in which $\sigma_1 = .05$, $\sigma_2 = .05$, $\rho = .5$, $\sigma_{\mu'} = .05$, $\sigma_{\mu} = .05$, $\rho_s = .0$, and $(\mu_{\mu} - A_1)/\sigma_{\mu'} = 0$, $(\mu_{\mu} - A_2)/\sigma_{\mu} = 2$.

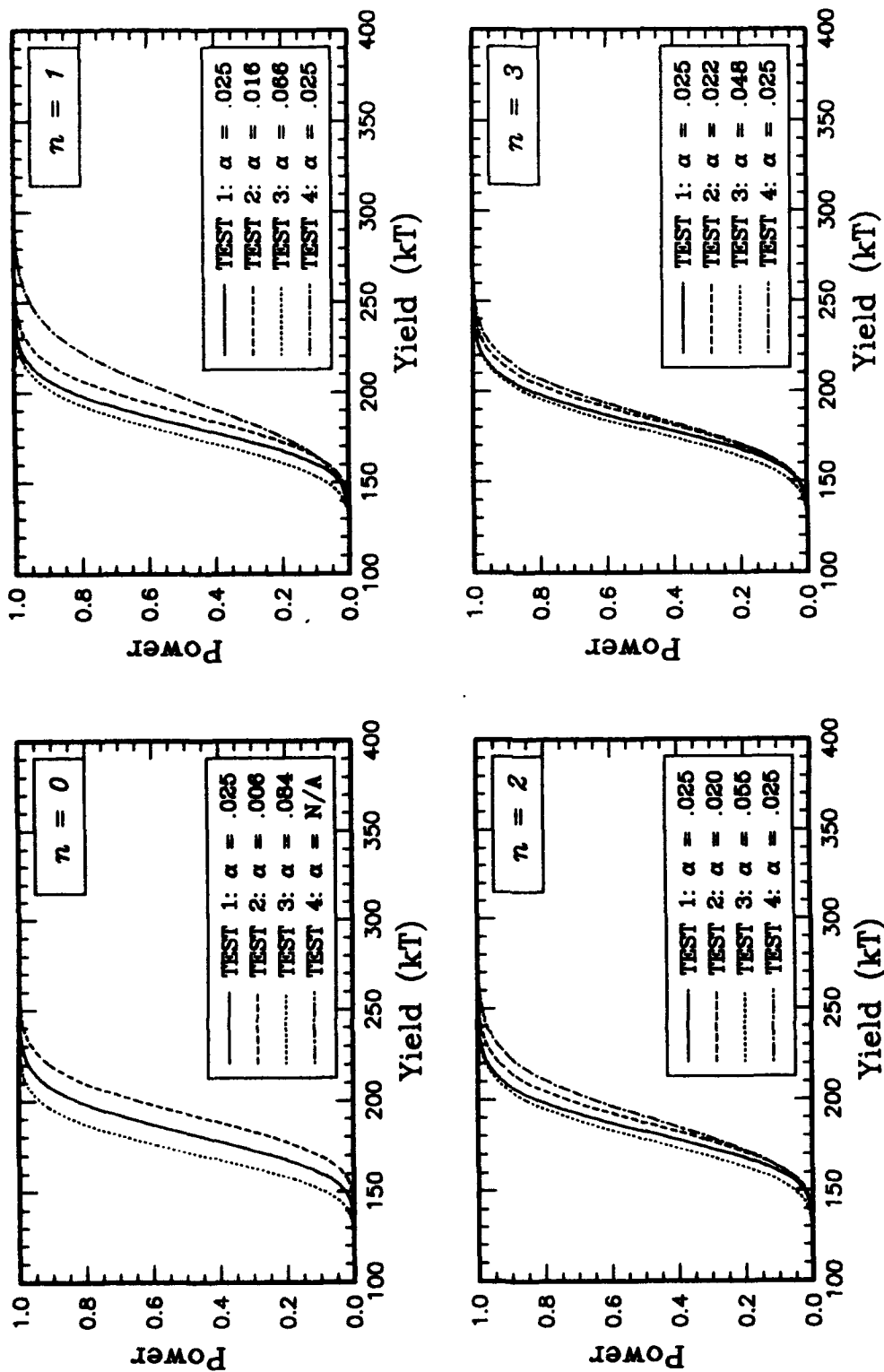


Figure 9c. Actual power curves of the four tests, as functions of yield, for the case in which $\sigma_1 = .05$, $\sigma_2 = .05$, $\rho = .5$, $\sigma_w = .05$, $\sigma_{\theta} = .05$, $\rho_{\theta} = .0$, and $(\mu_w - A_1)/\sigma_w = 0$, $(\mu_{\theta} - A_2)/\sigma_{\theta} = -2$.

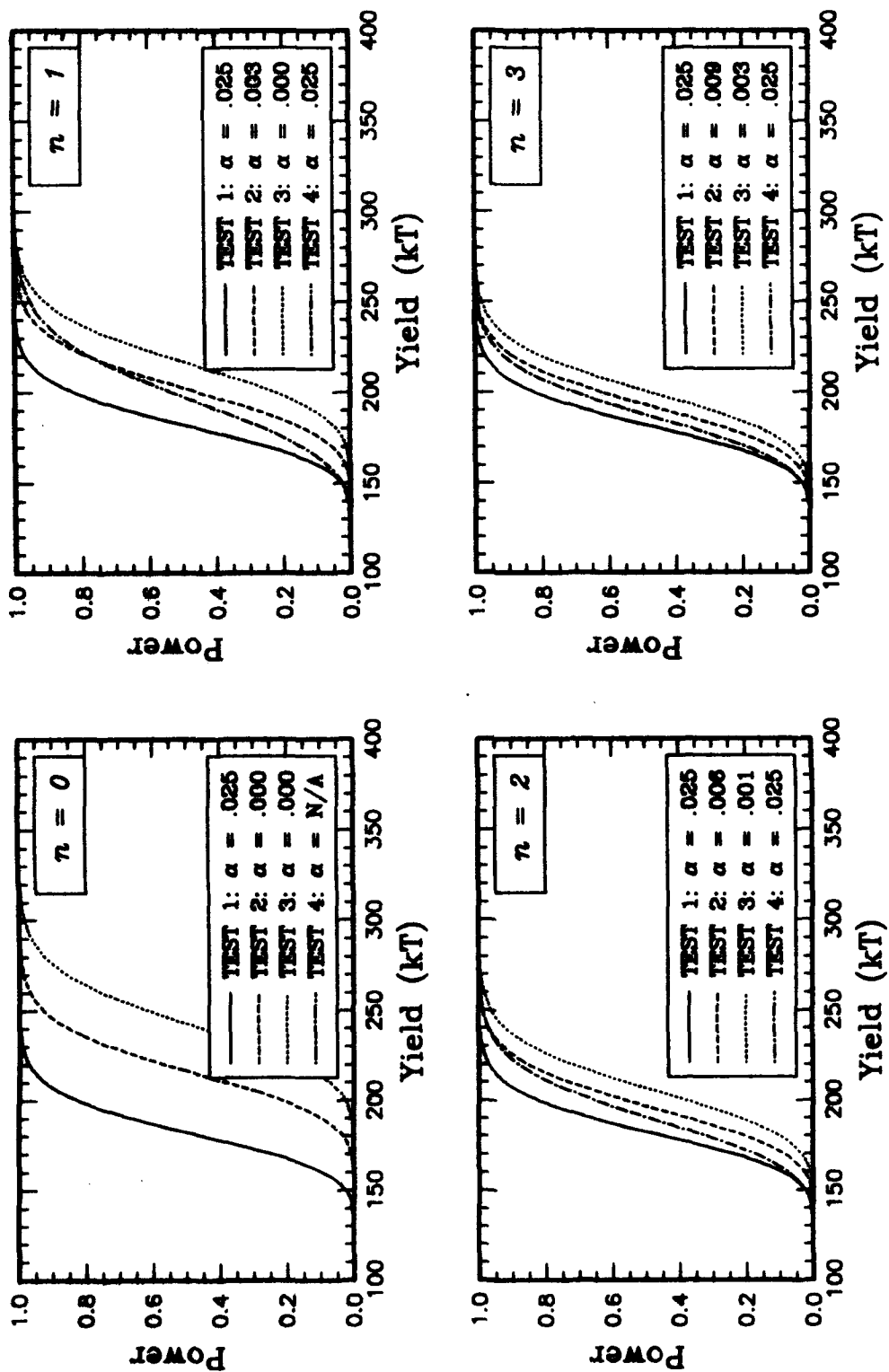


Figure 9d. Actual power curves of the four tests, as functions of yield, for the case in which $\sigma_1 = .05$, $\sigma_2 = .05$, $\rho = .5$, $\sigma_w = .05$, $\sigma_{\mu} = .05$, $\rho_s = .0$, and $(\mu_w - A_1)/\sigma_w = 2$, $(\mu_w - A_2)/\sigma_w = 2$.

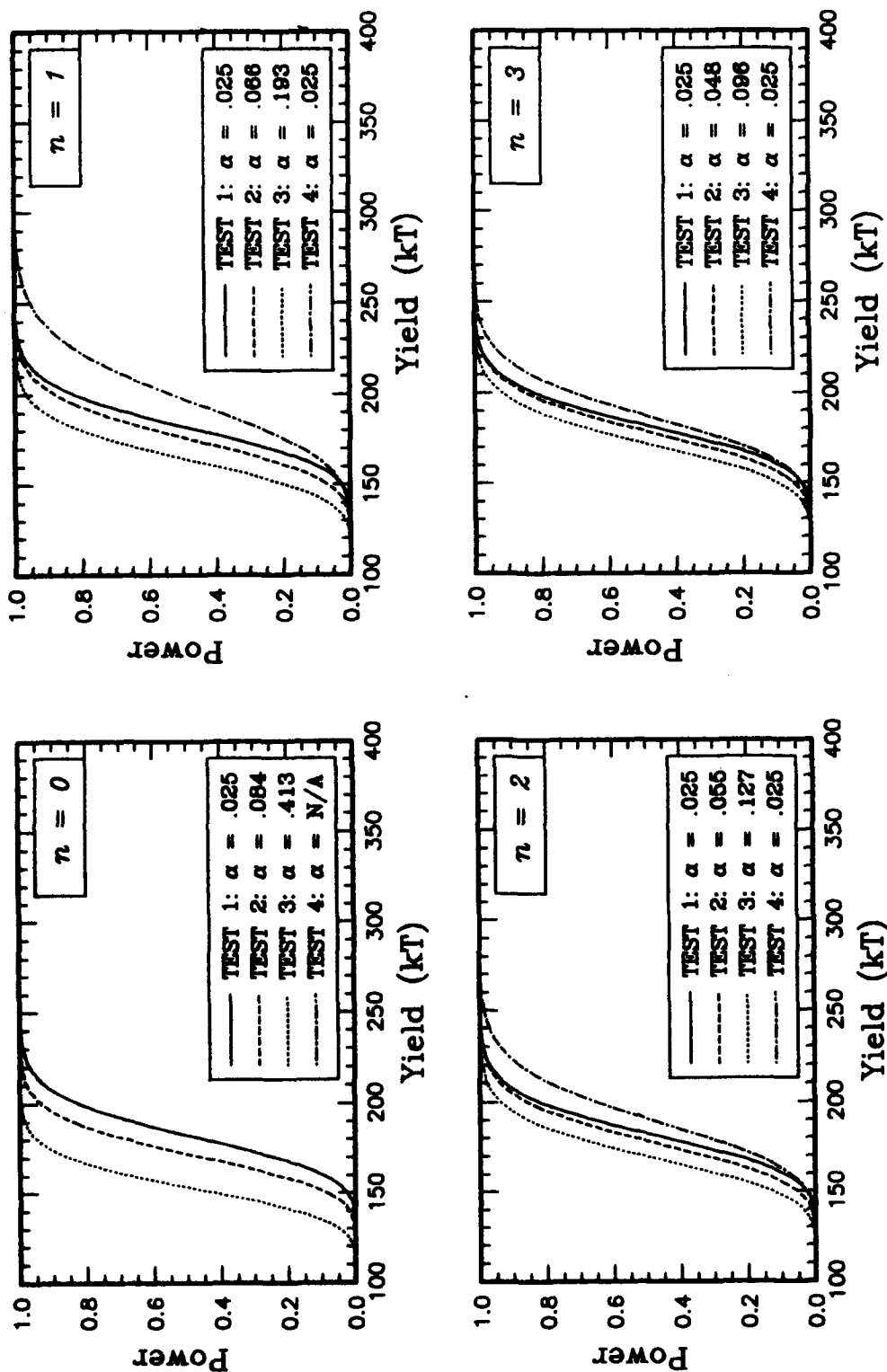


Figure 9e. Actual power curves of the four tests, as functions of yield, for the case in which $\sigma_1 = .05$, $\sigma_2 = .05$, $\rho = .5$, $\sigma_{\epsilon} = .05$, $\sigma_{\delta} = .05$, $\rho_{\epsilon} = .0$, and $(\mu_{\epsilon} - A_1)/\sigma_{\epsilon} = -2$, $(\mu_{\delta} - A_2)/\sigma_{\delta} = -2$.

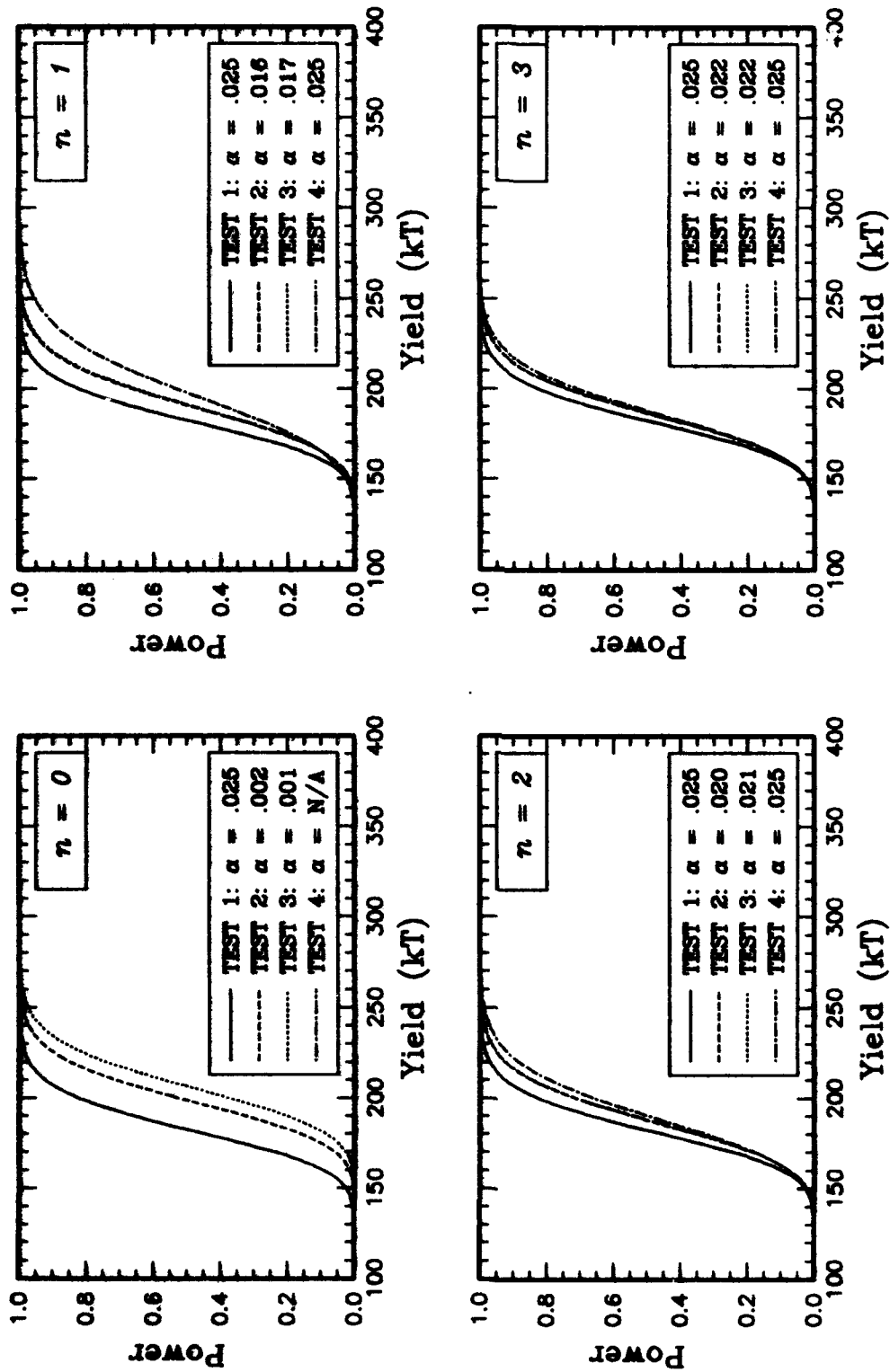


Figure 10a. Actual power curves of the four tests, as functions of yield, for the case in which $\sigma_1 = .05$, $\sigma_2 = .05$, $\rho = .5$, $\sigma_{\mu'} = .05$, $\sigma_{\sigma} = .10$, $\rho_{\sigma} = .0$, and $(\mu_{\sigma} - A_1)/\sigma_{\sigma} = 0$, $(\mu_{\sigma} - A_2)/\sigma_{\sigma} = 0$.

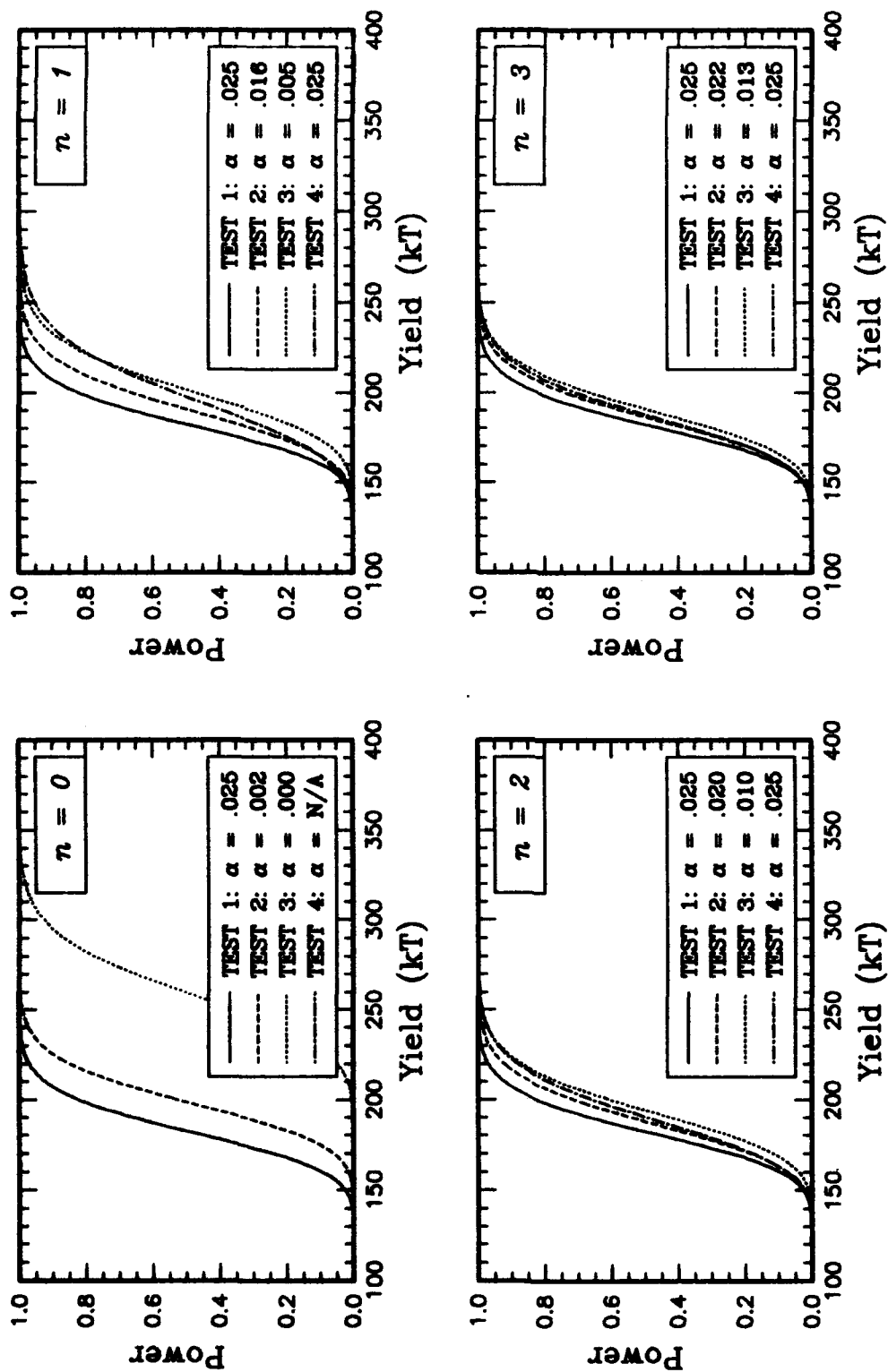


Figure 10b. Actual power curves of the four tests, as functions of yield, for the case in which $\sigma_1 = .05$, $\sigma_2 = .05$, $\rho = .5$, $\sigma_{\mu} = .05$, $\sigma_{\lambda} = .10$, $\rho_s = .0$, and $(\mu_{\mu} - A_1)/\sigma_{\mu} = 0$, $(\mu_{\lambda} - A_2)/\sigma_{\lambda} = 2$.

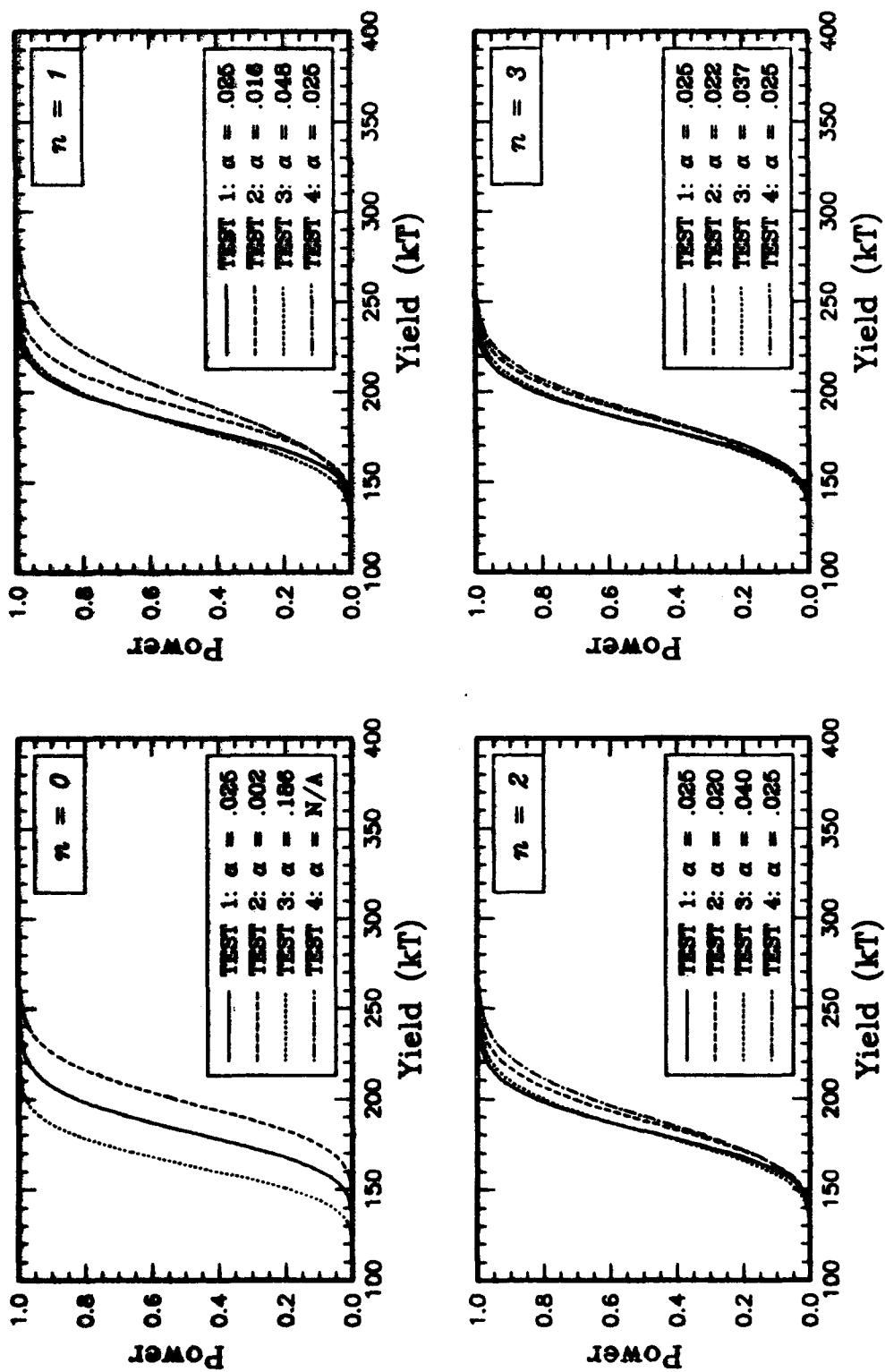


Figure 10c. Actual power curves of the four tests, as functions of yield, for the case in which $\sigma_1 = .05$, $\sigma_2 = .05$, $\rho = .5$, $\sigma_{\mu} = .05$, $\sigma_{\sigma} = .10$, $\rho_{\sigma} = .0$, and $(\mu_{\mu} - A_1)/\sigma_{\mu} = 0$, $(\mu_{\sigma} - A_2)/\sigma_{\sigma} = -2$.

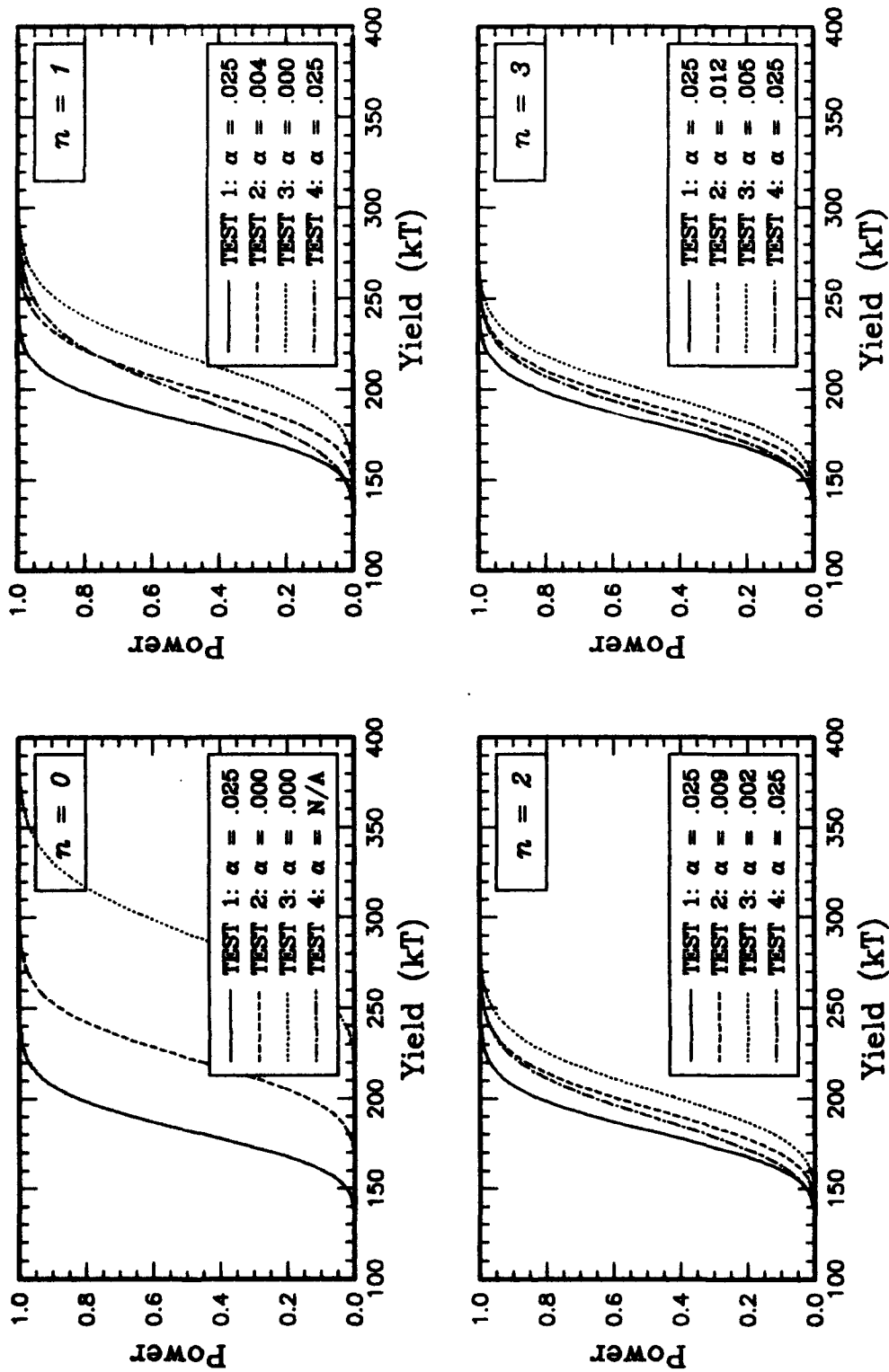


Figure 10d. Actual power curves of the four tests, as functions of yield, for the case in which $\sigma_1 = .05$, $\sigma_2 = .05$, $\rho = .5$, $\sigma_{A_1} = .05$, $\sigma_{A_2} = .10$, $\rho_0 = .0$, and $(\mu_{A_1} - A_1)/\sigma_{A_1} = 2$, $(\mu_{A_2} - A_2)/\sigma_{A_2} = 2$.

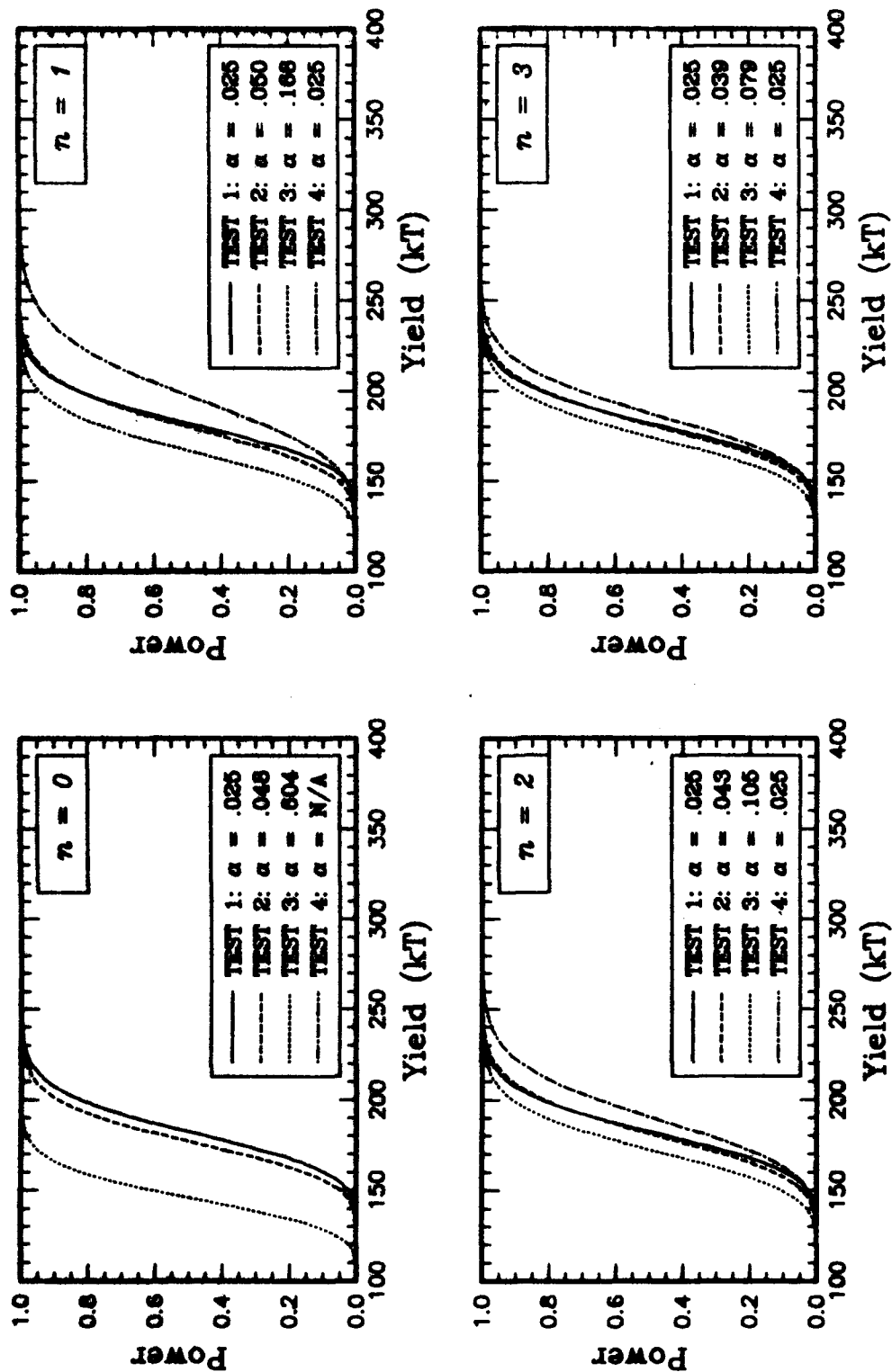


Figure 10e. Actual power curves of the four tests, as functions of yield, for the case in which $\sigma_1 = .05$, $\sigma_2 = .05$, $\rho = .5$, $\sigma_{\mu} = .05$, $\sigma_{\sigma} = .10$, $\rho_{\sigma} = .0$, and $(\mu_{\sigma} - A_1)/\sigma_{\sigma} = -2$, $(\mu_{\sigma} - A_2)/\sigma_{\sigma} = -2$.

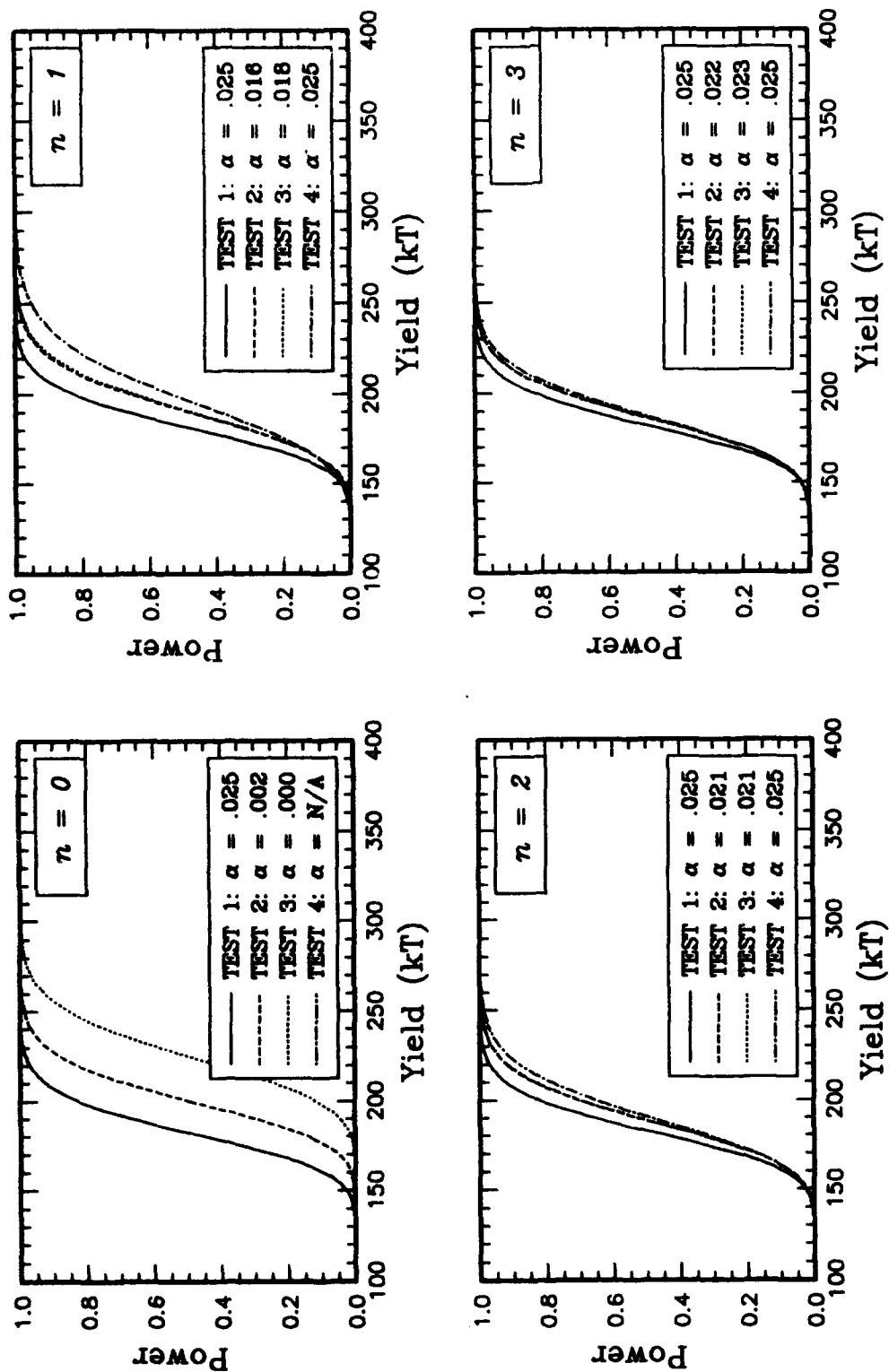


Figure 11a. Actual power curves of the four tests, as functions of yield, for the case in which $\sigma_1 = .05$, $\sigma_2 = .05$, $\rho = .5$, $\sigma_{A'} = .15$, $\rho_s = .0$, and $(\mu_{A'} - A_1)/\sigma_{A'} = 0$, $(\mu_{A_2} - A_2)/\sigma_{A_2} = 0$.

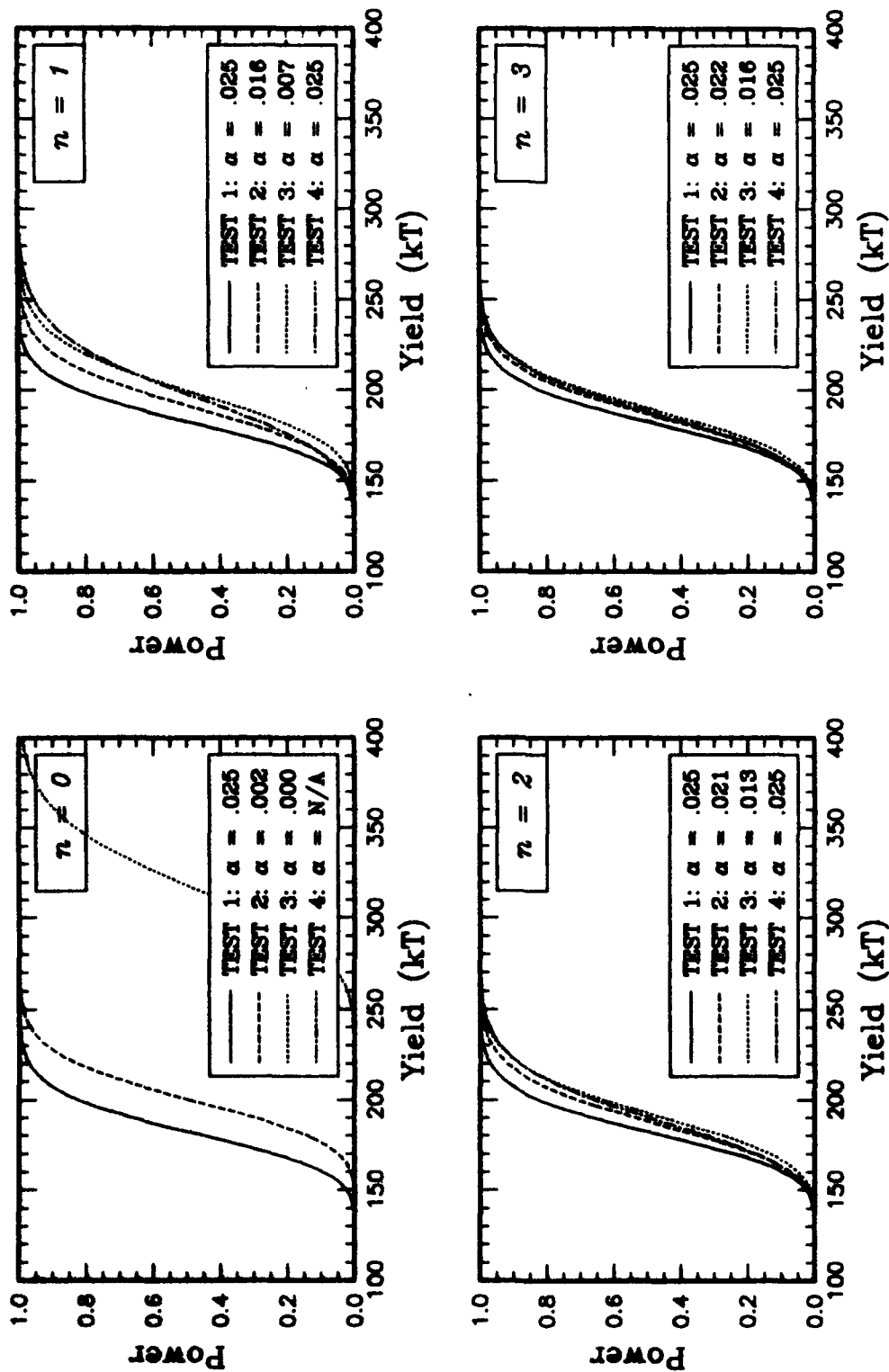


Figure 11b. Actual power curves of the four tests, as functions of yield, for the case in which $\sigma_1 = .05$, $\sigma_2 = .05$, $\rho = .5$, $\sigma_w = .05$, $\sigma_s = .15$, $\rho_s = .0$, and $(\mu_w - A_1)/\sigma_w = 0$, $(\mu_s - A_2)/\sigma_s = 2$.

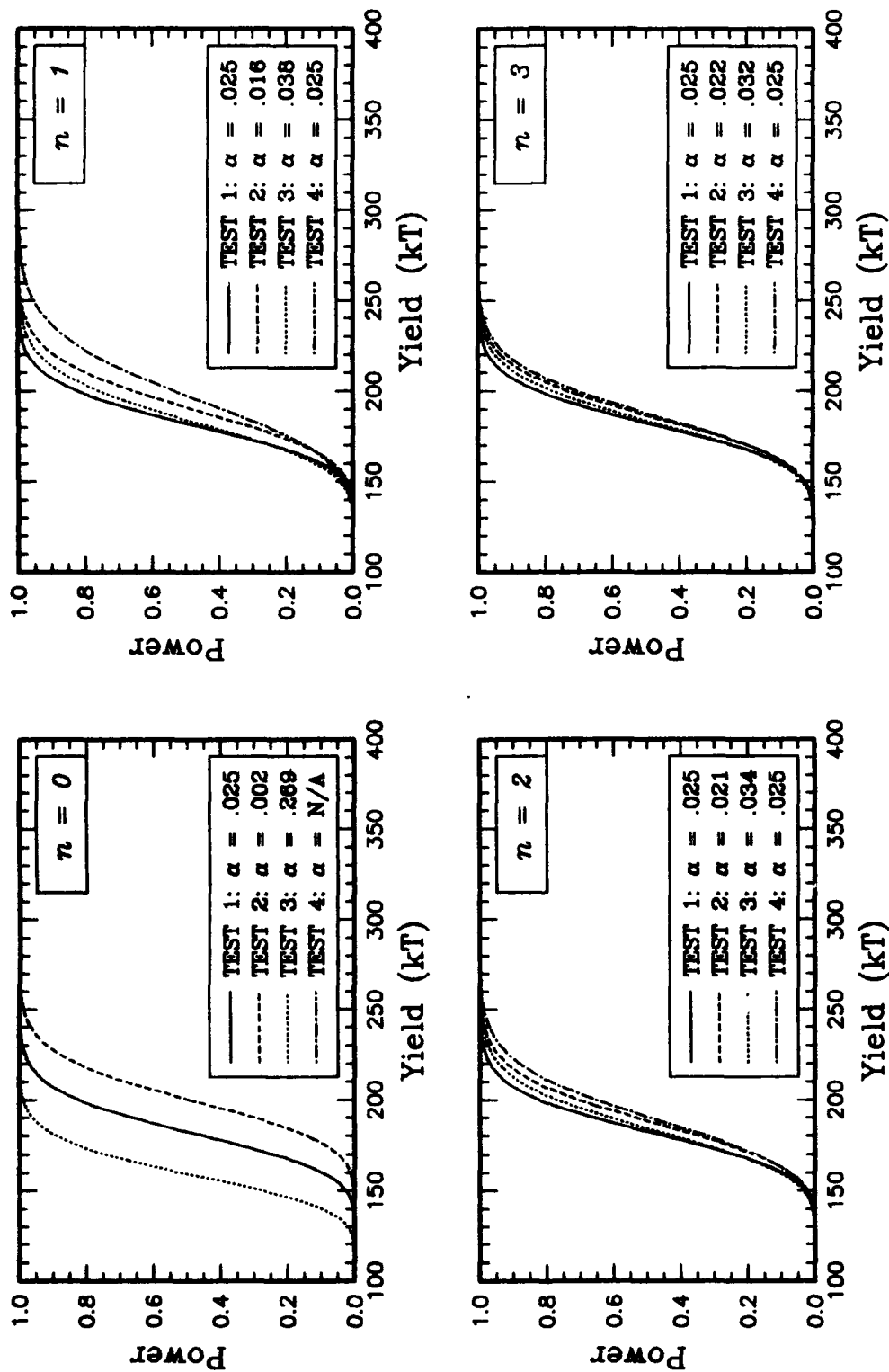


Figure 11c. Actual power curves of the four tests, as functions of yield, for the case in which $\sigma_1 = .05$, $\sigma_2 = .05$, $\rho = .5$, $\sigma_{A_1} = .05$, $\sigma_{A_2} = .15$, $\rho_s = .0$, and $(\mu_{A_1} - A_1)/\sigma_{A_1} = 0$, $(\mu_{A_2} - A_2)/\sigma_{A_2} = -2$.

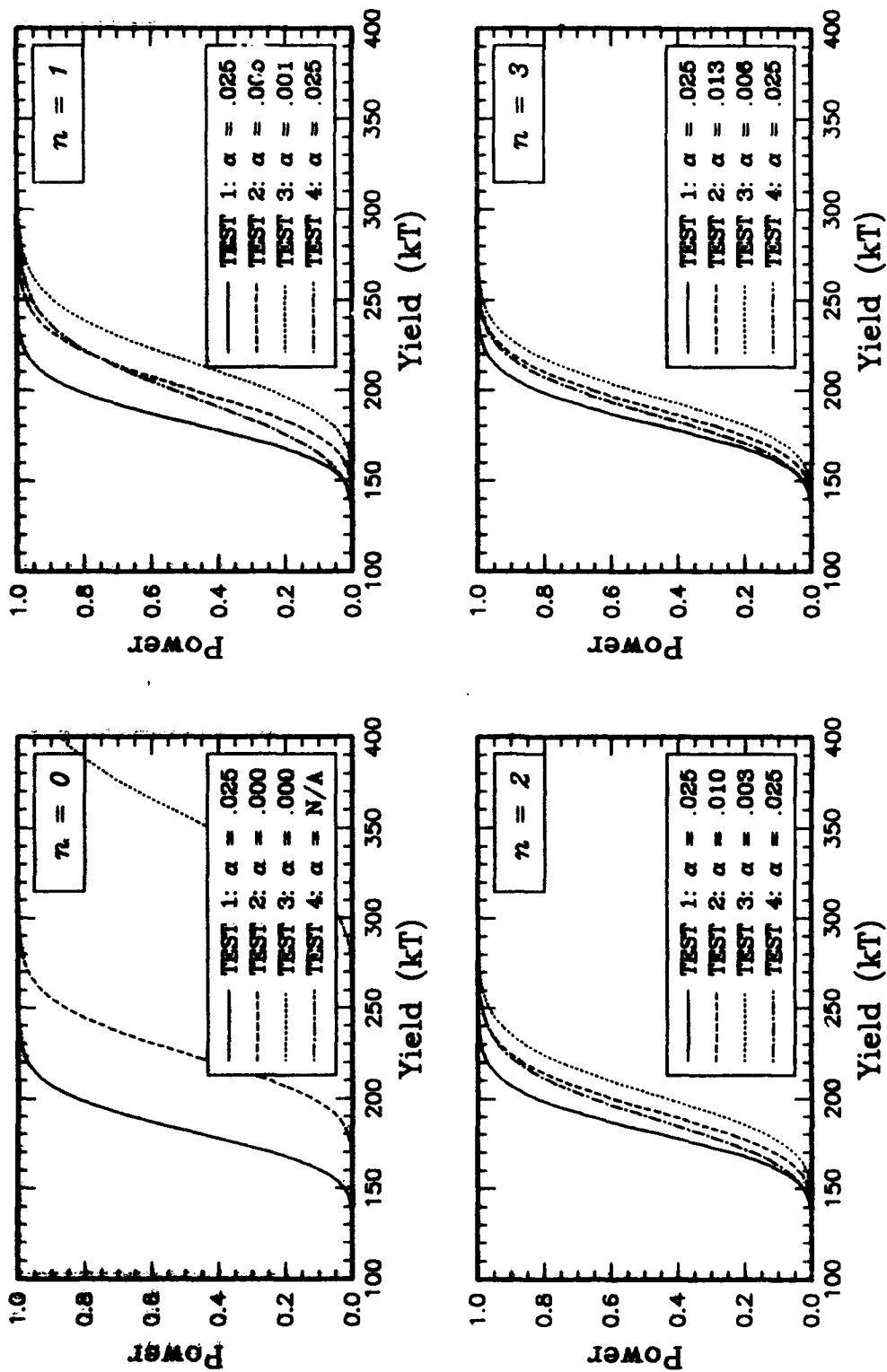


Figure 11d. Actual power curves of the four tests, as functions of yield, for the case in which $\sigma_1 = .05$, $\sigma_2 = .05$, $\rho = .5$, $\sigma_{\mu} = .05$, $\sigma_{\sigma} = .15$, $\rho_{\sigma} = .0$, and $(\mu_{\mu} - A_1)/\sigma_{\mu} = 2$, $(\mu_{\sigma} - A_2)/\sigma_{\sigma} = 2$.

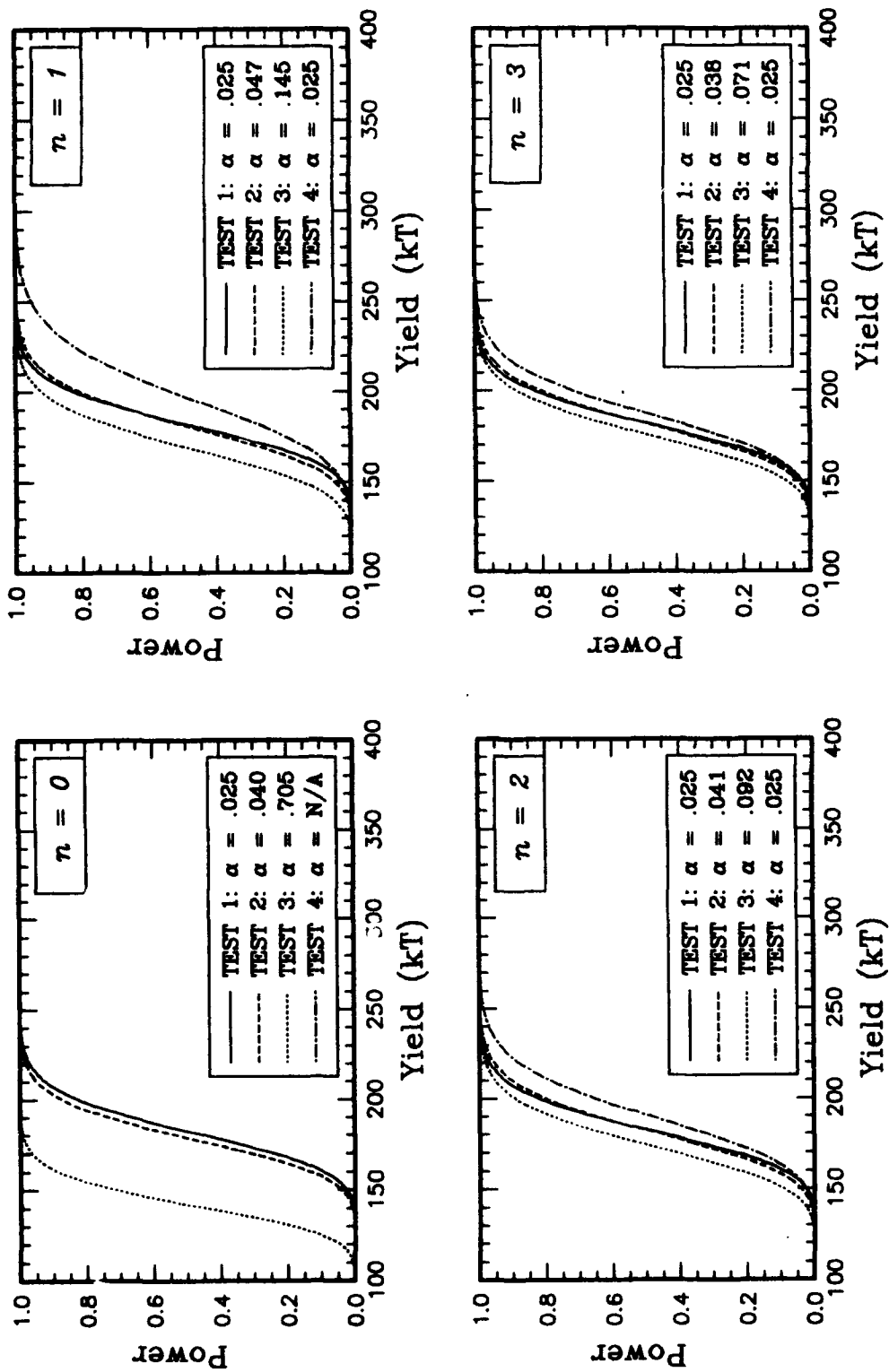


Figure 11e. Actual power curves of the four tests, as functions of yield, for the case in which $\sigma_1 = .05$, $\sigma_2 = .05$, $\rho = .5$, $\sigma_{\mu} = .05$, $\sigma_{\sigma} = .15$, $\rho_{\sigma} = .0$, and $(\mu_{\mu} - A_1)/\sigma_{\mu} = -2$, $(\mu_{\sigma} - A_2)/\sigma_{\sigma} = -2$.

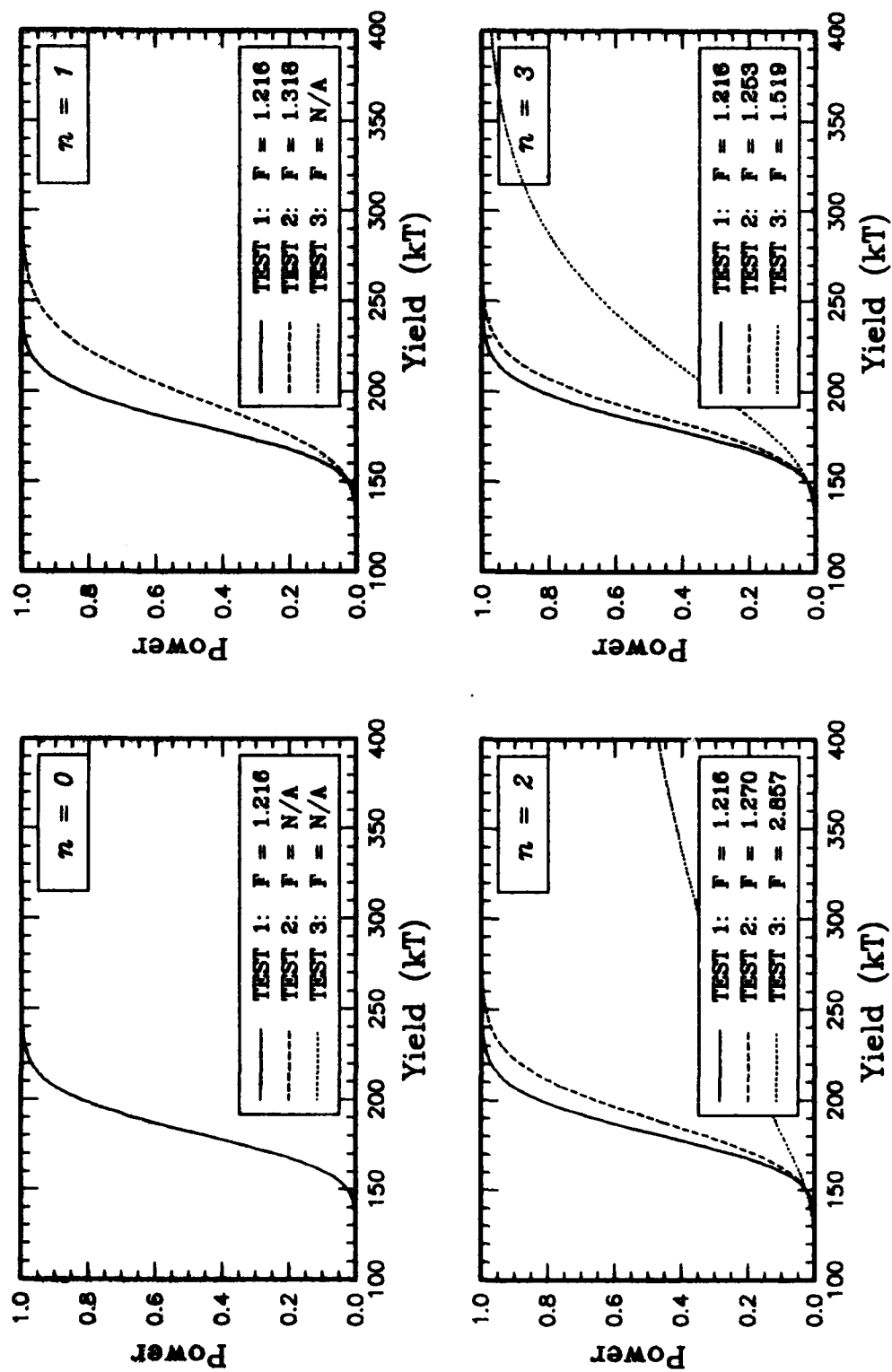


Figure 12. Power curves of three tests based on all parameters known (solid), unknown intercepts only (dashed), and unknown intercepts and covariance matrix of the random errors (dotted) for the case in which $\sigma_1 = .05$, $\sigma_2 = .05$, $\rho = .5$.

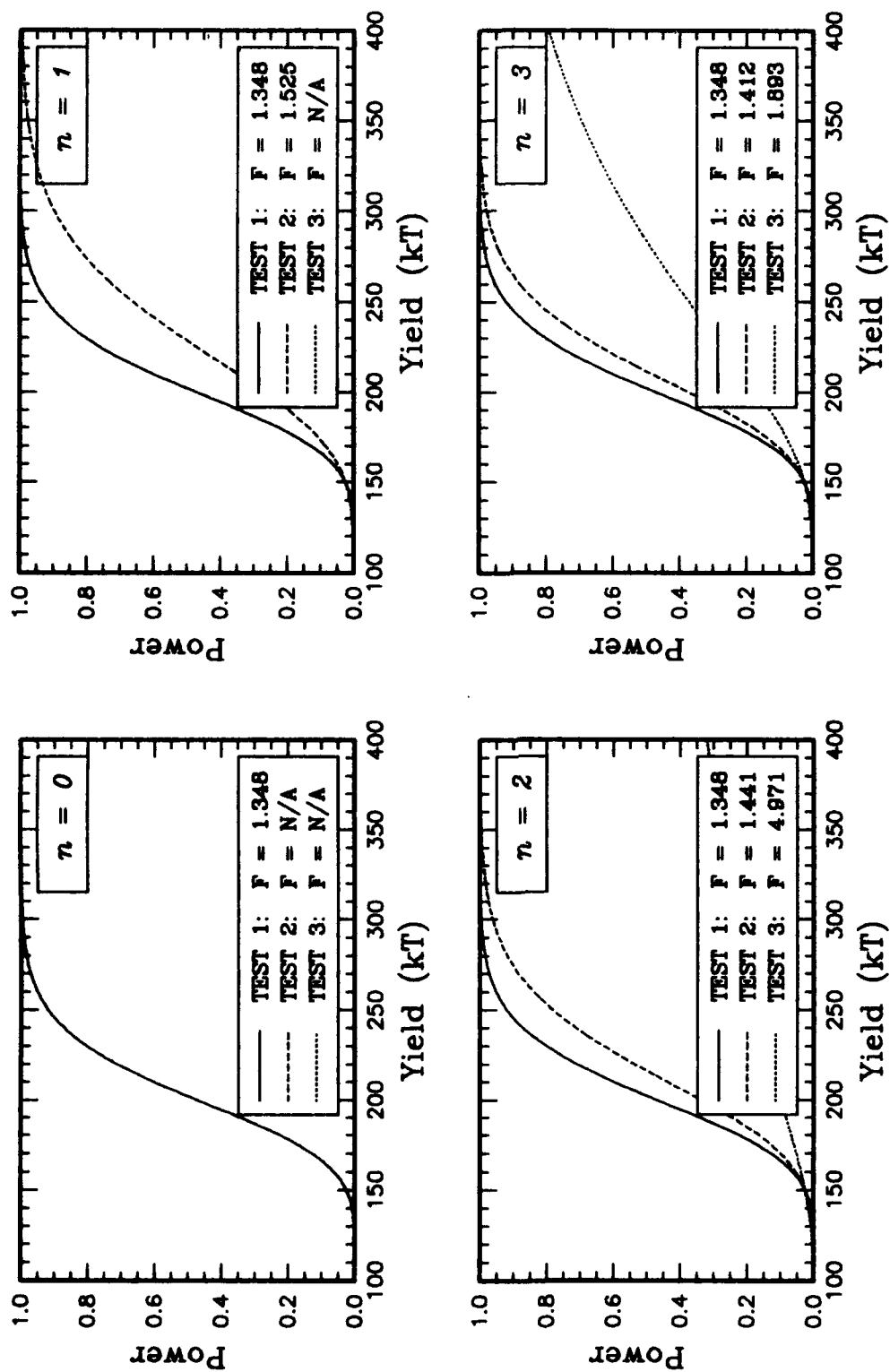


Figure 13. Power curves of three tests based on all parameters known (solid), unknown intercepts only (dashed), and unknown intercepts and covariance matrix of the random errors (dotted) for the case in which $\sigma_1 = .05$, $\sigma_2 = .10$, $\rho = .5$.

DISTRIBUTION LIST

Prof. Thomas Ahrens
Seismological Lab, 252-21
Division of Geological & Planetary Sciences
California Institute of Technology
Pasadena, CA 91125

Prof. Keiiti Aki
Center for Earth Sciences
University of Southern California
University Park
Los Angeles, CA 90089-0741

Prof. Shelton Alexander
Geosciences Department
403 Deike Building
The Pennsylvania State University
University Park, PA 16802

Dr. Ralph Alewine, III
DARPA/NMRO
3701 North Fairfax Drive
Arlington, VA 22203-1714

Prof. Charles B. Archambeau
CIRES
University of Colorado
Boulder, CO 80309

Dr. Thomas C. Bache, Jr.
Science Applications Int'l Corp.
10260 Campus Point Drive
San Diego, CA 92121 (2 copies)

Prof. Muawia Barazangi
Institute for the Study of the Continent
Cornell University
Ithaca, NY 14853

Dr. Jeff Barker
Department of Geological Sciences
State University of New York
at Binghamton
Vestal, NY 13901

Dr. Douglas R. Baumgardt
ENSCO, Inc
5400 Port Royal Road
Springfield, VA 22151-2388

Dr. Susan Beck
Department of Geosciences
Building #77
University of Arizona
Tucson, AZ 85721

Dr. T.J. Bennett
S-CUBED
A Division of Maxwell Laboratories
11800 Sunrise Valley Drive, Suite 1212
Reston, VA 22091

Dr. Robert Blandford
AFTAC/TT, Center for Seismic Studies
1300 North 17th Street
Suite 1450
Arlington, VA 22209-2308

Dr. G.A. Bollinger
Department of Geological Sciences
Virginia Polytechnical Institute
21044 Derring Hall
Blacksburg, VA 24061

Dr. Stephen Bratt
Center for Seismic Studies
1300 North 17th Street
Suite 1450
Arlington, VA 22209-2308

Dr. Lawrence Burdick
Woodward-Clyde Consultants
566 El Dorado Street
Pasadena, CA 91109-3245

Dr. Robert Burrige
Schlumberger-Doll Research Center
Old Quarry Road
Ridgefield, CT 06877

Dr. Jerry Carter
Center for Seismic Studies
1300 North 17th Street
Suite 1450
Arlington, VA 22209-2308

Dr. Eric Chael
Division 9241
Sandia Laboratory
Albuquerque, NM 87185

Prof. Vernon F. Cormier
Department of Geology & Geophysics
U-45, Room 207
University of Connecticut
Storrs, CT 06268

Prof. Steven Day
Department of Geological Sciences
San Diego State University
San Diego, CA 92182

Marvin Denny
U.S. Department of Energy
Office of Arms Control
Washington, DC 20585

Dr. Cliff Frolich
Institute of Geophysics
8701 North Mopac
Austin, TX 78759

Dr. Zoltan Der
ENSCO, Inc.
5400 Port Royal Road
Springfield, VA 22151-2388

Dr. Holly Given
IGPP, A-025
Scripps Institute of Oceanography
University of California, San Diego
La Jolla, CA 92093

Prof. Adam Dziewonski
Hoffman Laboratory, Harvard University
Dept. of Earth Atmos. & Planetary Sciences
20 Oxford Street
Cambridge, MA 02138

Dr. Jeffrey W. Given
SAIC
10260 Campus Point Drive
San Diego, CA 92121

Prof. John Ebel
Department of Geology & Geophysics
Boston College
Chestnut Hill, MA 02167

Dr. Dale Glover
Defense Intelligence Agency
ATTN: ODT-1B
Washington, DC 20301

Eric Fielding
SNEE Hall
INSTOC
Cornell University
Ithaca, NY 14853

Dr. Indra Gupta
Teledyne Geotech
314 Montgomery Street
Alexandria, VA 22314

Dr. Mark D. Fisk
Mission Research Corporation
735 State Street
P.O. Drawer 719
Santa Barbara, CA 93102

Dan N. Hagedorn
Pacific Northwest Laboratories
Battelle Boulevard
Richland, WA 99352

Prof Stanley Flatté
Applied Sciences Building
University of California, Santa Cruz
Santa Cruz, CA 95064

Dr. James Hannon
Lawrence Livermore National Laboratory
P.O. Box 808
L-205
Livermore, CA 94550

Dr. John Foley
NER-Geo Sciences
1100 Crown Colony Drive
Quincy, MA 02169

Dr. Roger Hansen
HQ AFTAC/TTR
Patrick AFB, FL 32925-6001

Prof. Donald Forsyth
Department of Geological Sciences
Brown University
Providence, RI 02912

Prof. David G. Harkrider
Seismological Laboratory
Division of Geological & Planetary Sciences
California Institute of Technology
Pasadena, CA 91125

Dr. Art Frankel
U.S. Geological Survey
922 National Center
Reston, VA 22092

Prof. Danny Harvey
CIRES
University of Colorado
Boulder, CO 80309

Prof. Donald V. Helmberger
Seismological Laboratory
Division of Geological & Planetary Sciences
California Institute of Technology
Pasadena, CA 91125

Prof. Eugene Herrin
Institute for the Study of Earth and Man
Geophysical Laboratory
Southern Methodist University
Dallas, TX 75275

Prof. Robert B. Herrmann
Department of Earth & Atmospheric Sciences
St. Louis University
St. Louis, MO 63156

Prof. Lane R. Johnson
Seismographic Station
University of California
Berkeley, CA 94720

Prof. Thomas H. Jordan
Department of Earth, Atmospheric &
Planetary Sciences
Massachusetts Institute of Technology
Cambridge, MA 02139

Prof. Alan Kafka
Department of Geology & Geophysics
Boston College
Chestnut Hill, MA 02167

Robert C. Kemerait
ENSCO, Inc.
445 Pineda Court
Melbourne, FL 32940

Dr. Max Koontz
U.S. Dept. of Energy/DP 5
Forrestal Building
1000 Independence Avenue
Washington, DC 20585

Dr. Richard LaCoss
MIT Lincoln Laboratory, M-200B
P.O. Box 73
Lexington, MA 02173-0073

Dr. Fred K. Lamb
University of Illinois at Urbana-Champaign
Department of Physics
1110 West Green Street
Urbana, IL 61801

Prof. Charles A. Langston
Geosciences Department
403 Deike Building
The Pennsylvania State University
University Park, PA 16802

Jim Lawson, Chief Geophysicist
Oklahoma Geological Survey
Oklahoma Geophysical Observatory
P.O. Box 8
Leonard, OK 74043-0008

Prof. Thorne Lay
Institute of Tectonics
Earth Science Board
University of California, Santa Cruz
Santa Cruz, CA 95064

Dr. William Leith
U.S. Geological Survey
Mail Stop 928
Reston, VA 22092

Mr. James F. Lewkowicz
Phillips Laboratory/GPEH
Hanscom AFB, MA 01731-5000(2 copies)

Mr. Alfred Lieberman
ACDA/VI-OA State Department Building
Room 5726
320-21st Street, NW
Washington, DC 20451

Prof. L. Timothy Long
School of Geophysical Sciences
Georgia Institute of Technology
Atlanta, GA 30332

Dr. Randolph Martin, III
New England Research, Inc.
76 Olcott Drive
White River Junction, VT 05001

Dr. Robert Masse
Denver Federal Building
Box 25046, Mail Stop 967
Denver, CO 80225

Dr. Gary McCartor
Department of Physics
Southern Methodist University
Dallas, TX 75275

Prof. Thomas V. McEvilly
Seismographic Station
University of California
Berkeley, CA 94720

Dr. Art McGarr
U.S. Geological Survey
Mail Stop 977
U.S. Geological Survey
Menlo Park, CA 94025

Dr. Keith L. McLaughlin
S-CUBED
A Division of Maxwell Laboratory
P.O. Box 1620
La Jolla, CA 92038-1620

Stephen Miller & Dr. Alexander Florence
SRI International
333 Ravenswood Avenue
Box AF 116
Menlo Park, CA 94025-3493

Prof. Bernard Minster
IGPP, A-025
Scripps Institute of Oceanography
University of California, San Diego
La Jolla, CA 92093

Prof. Brian J. Mitchell
Department of Earth & Atmospheric Sciences
St. Louis University
St. Louis, MO 63156

Mr. Jack Murphy
S-CUBED
A Division of Maxwell Laboratory
11800 Sunrise Valley Drive, Suite 1212
Reston, VA 22091 (2 Copies)

Dr. Keith K. Nakanishi
Lawrence Livermore National Laboratory
L-025
P.O. Box 808
Livermore, CA 94550

Dr. Carl Newton
Los Alamos National Laboratory
P.O. Box 1663
Mail Stop C335, Group ESS-3
Los Alamos, NM 87545

Dr. Bao Nguyen
HQ AFTAC/TTR
Patrick AFB, FL 32925-6001

Prof. John A. Orcutt
IGPP, A-025
Scripps Institute of Oceanography
University of California, San Diego
La Jolla, CA 92093

Prof. Jeffrey Park
Kline Geology Laboratory
P.O. Box 6666
New Haven, CT 06511-8130

Dr. Howard Patton
Lawrence Livermore National Laboratory
L-025
P.O. Box 808
Livermore, CA 94550

Dr. Frank Pilotte
HQ AFTAC/TT
Patrick AFB, FL 32925-6001

Dr. Jay J. Pulli
Radix Systems, Inc.
2 Taft Court, Suite 203
Rockville, MD 20850

Dr. Robert Reinke
ATTN: FCTVTD
Field Command
Defense Nuclear Agency
Kirtland AFB, NM 87115

Prof. Paul G. Richards
Lamont-Doherty Geological Observatory
of Columbia University
Palisades, NY 10964

Mr. Wilmer Rivers
Teledyne Geotech
314 Montgomery Street
Alexandria, VA 22314

Dr. George Rothe
HQ AFTAC/TTR
Patrick AFB, FL 32925-6001

Dr. Alan S. Ryall, Jr.
DARPA/NMRO
3701 North Fairfax Drive
Arlington, VA 22209-1714

Dr. Richard Sailor
TASC, Inc.
55 Walkers Brook Drive
Reading, MA 01867

Prof. Charles G. Sammis
Center for Earth Sciences
University of Southern California
University Park
Los Angeles, CA 90089-0741

Prof. Christopher H. Scholz
Lamont-Doherty Geological Observatory
of Columbia University
Palisades, CA 10964

Dr. Susan Schwartz
Institute of Tectonics
1156 High Street
Santa Cruz, CA 95064

Secretary of the Air Force
(SAFRD)
Washington, DC 20330

Office of the Secretary of Defense
DDR&E
Washington, DC 20330

Thomas J. Sereno, Jr.
Science Application Int'l Corp.
10260 Campus Point Drive
San Diego, CA 92121

Dr. Michael Shore
Defense Nuclear Agency/SPSS
6801 Telegraph Road
Alexandria, VA 22310

Dr. Matthew Sibol
Virginia Tech
Seismological Observatory
4044 Derring Hall
Blacksburg, VA 24061-0420

Prof. David G. Simpson
IRIS, Inc.
1616 North Fort Myer Drive
Suite 1440
Arlington, VA 22209

Donald L. Springer
Lawrence Livermore National Laboratory
L-025
P.O. Box 808
Livermore, CA 94550

Dr. Jeffrey Stevens
S-CUBED
A Division of Maxwell Laboratory
P.O. Box 1620
La Jolla, CA 92038-1620

Lt. Col. Jim Stobie
ATTN: AFOSR/NL
Bolling AFB
Washington, DC 20332-6448

Prof. Brian Stump
Institute for the Study of Earth & Man
Geophysical Laboratory
Southern Methodist University
Dallas, TX 75275

Prof. Jeremiah Sullivan
University of Illinois at Urbana-Champaign
Department of Physics
1110 West Green Street
Urbana, IL 61801

Prof. L. Sykes
Lamont-Doherty Geological Observatory
of Columbia University
Palisades, NY 10964

Dr. David Taylor
ENSCO, Inc.
445 Pineda Court
Melbourne, FL 32940

Dr. Steven R. Taylor
Los Alamos National Laboratory
P.O. Box 1663
Mail Stop C335
Los Alamos, NM 87545

Prof. Clifford Thurber
University of Wisconsin-Madison
Department of Geology & Geophysics
1215 West Dayton Street
Madison, WS 53706

Prof. M. Nafi Toksoz
Earth Resources Lab
Massachusetts Institute of Technology
42 Carleton Street
Cambridge, MA 02142

Dr. Larry Turnbull
CIA-OSWR/NED
Washington, DC 20505

DARPA/RMO/SECURITY OFFICE
3701 North Fairfax Drive
Arlington, VA 22203-1714

Dr. Gregory van der Vink
IRIS, Inc.
1616 North Fort Myer Drive
Suite 1440
Arlington, VA 22209

HQ DNA
ATTN: Technical Library
Washington, DC 20305

Dr. Karl Veith
EG&G
5211 Auth Road
Suite 240
Suitland, MD 20746

Defense Intelligence Agency
Directorate for Scientific & Technical Intelligence
ATTN: DTIB
Washington, DC 20340-6158

Prof. Terry C. Wallace
Department of Geosciences
Building #77
University of Arizona
Tucson, AZ 85721

Defense Technical Information Center
Cameron Station
Alexandria, VA 22314 (2 Copies)

Dr. Thomas Weaver
Los Alamos National Laboratory
P.O. Box 1663
Mail Stop C335
Los Alamos, NM 87545

TACTEC
Battelle Memorial Institute
505 King Avenue
Columbus, OH 43201 (Final Report)

Dr. William Wortman
Mission Research Corporation
8560 Cinderbed Road
Suite 700
Newington, VA 22122

Phillips Laboratory
ATTN: XPG
Hanscom AFB, MA 01731-5000

Prof. Francis T. Wu
Department of Geological Sciences
State University of New York
at Binghamton
Vestal, NY 13901

Phillips Laboratory
ATTN: GPE
Hanscom AFB, MA 01731-5000

AFTAC/CA
(STINFO)
Patrick AFB, FL 32925-6001

Phillips Laboratory
ATTN: TSML
Hanscom AFB, MA 01731-5000

DARPA/PM
3701 North Fairfax Drive
Arlington, VA 22203-1714

Phillips Laboratory
ATTN: SUL
Kirtland, NM 87117 (2 copies)

DARPA/RMO/RETRIEVAL
3701 North Fairfax Drive
Arlington, VA 22203-1714

Dr. Michel Bouchon
I.R.I.G.M.-B.P. 68
38402 St. Martin D'Heres
Cedex, FRANCE

Dr. Michel Campillo
Observatoire de Grenoble
I.R.I.G.M.-B.P. 53
38041 Grenoble, FRANCE

Dr. Jorg Schlittenhardt
Federal Institute for Geosciences & Nat'l Res.
Postfach 510153
D-3000 Hannover 51, GERMANY

Dr. Kin Yip Chun
Geophysics Division
Physics Department
University of Toronto
Ontario, CANADA

Dr. Johannes Schweitzer
Institute of Geophysics
Ruhr University/Bochum
P.O. Box 1102148
4360 Bochum 1, GERMANY

Prof. Hans-Peter Harjes
Institute for Geophysics
Ruhr University/Bochum
P.O. Box 102148
4630 Bochum 1, GERMANY

Prof. Eystein Husebye
NTNF/NORSAR
P.O. Box 51
N-2007 Kjeller, NORWAY

David Jepsen
Acting Head, Nuclear Monitoring Section
Bureau of Mineral Resources
Geology and Geophysics
G.P.O. Box 378, Canberra, AUSTRALIA

Ms. Eva Johannisson
Senior Research Officer
National Defense Research Inst.
P.O. Box 27322
S-102 54 Stockholm, SWEDEN

Dr. Peter Marshall
Procurement Executive
Ministry of Defense
Blacknest, Brimpton
Reading FG7-FRS, UNITED KINGDOM

Dr. Bernard Massinon, Dr. Pierre Mechler
Societe Radiomana
27 rue Claude Bernard
75005 Paris, FRANCE (2 Copies)

Dr. Svein Mykkeltveit
NTNF/NORSAR
P.O. Box 51
N-2007 Kjeller, NORWAY (3 Copies)

Prof. Keith Priestley
University of Cambridge
Bullard Labs, Dept. of Earth Sciences
Madingley Rise, Madingley Road
Cambridge CB3 0EZ, ENGLAND